Final Report:

Image-Based Assessment of Habitat Quality in Marron Valley

Project conducted by:
Department of Geography
San Diego State University
5500 Campanile Drive
San Diego, CA 92182-4493

Report prepared by:
Lloyd Coulter, Jenny Williams, and Douglas Stow
San Diego State University

Report prepared for:
Keith Greer
City of San Diego
Planning Department
202 C Street, MS 5A
San Diego, CA 92101-3865

October 24, 2003

Table of Contents

Tables

Figures

Executive Summary

Remotely sensed imagery may significantly aid the City of San Diego (City) in managing natural lands of the Multiple Species Conservation Program (MSCP). The primary objective of this study was to investigate the utility of high resolution, multispectral imagery for quantifying the cover proportions of shrub, herbaceous, and bare ground cover within vegetation stands. The proportional distribution of these cover types may be an indicator of habitat quality. Mapping these cover types using remotely sensed imagery may enable frequent assessment of habitat conditions and changes in conditions over time. In addition, the project analyzed spectral signatures of vegetation stands dominated by native and non-native plant species, investigated the effect of fire and fire recovery on overall image brightness, and evaluated image segmentation techniques for semi-automated delineation of vegetation stands within multispectral imagery.

The study site for this project was the City property within Marron Valley. ADAR 5500 multispectral imagery was acquired in April and August of 2002, at 1 m spatial resolution. The multitemporal imagery was acquired and processed in a specific manner that yielded precise spatial co-registration between resulting ADAR 5500 mosaics. This level of spatial co-registration between the multitemporal image sets enabled pixel-level changes in vegetation phenology to be exploited for discriminating shrub from herbaceous cover.

Image classifications of shrub, herbaceous, and bare soil cover were generated using April and August single date imagery, and using a multitemporal data set combining imagery from April and August. Two techniques for image classification were evaluated for each image set: unsupervised classification and model-based classification using the ERDAS Expert Classifier. Image classifications were calibrated and validated by comparing image-derived estimates of cover to those field mapped by the City, on a per-vegetation stand basis. Overall image classification accuracy did not vary substantially between the different approaches, and image-derived cover proportions were generally within 20% of those field-estimated by the City. Results suggest that the most efficient, objective, and accurate technique for estimating shrub, herbaceous, and bare soil cover is likely to be through model-based image classification of multispectral imagery (and derived products) acquired in late July or August.

Spectral signatures were compiled from areas field mapped by the City as having high percentages of individual native and exotic species. The goal was to identify any unique spectral characteristics which may be utilized to detect and classify these plant species within multispectral imagery. However, the analysis of spectral signatures was limited due to the mixture of cover types present within the mapped vegetation stands, and significant conclusions could not be drawn.

The recovery of vegetation following fire and other disturbance agents is important to monitor, as it is directly related to the recovery of habitat within affected areas. The project team assessed whether or not fire affected areas have characteristically different spectral reflectance than non-fire affected areas and if airborne multispectral imagery could provide information on the status of fire recovery. Relationships between overall image brightness and the number of years since the last fire were tested for areas in Marron Valley known to have burned within the last 35

years. A quantitative measure was used to summarize overall image brightness for each burn unit. The strongest relationship between overall image brightness and number of years since last burn was found for the April ADAR data set. Over 40% of the variation in overall image brightness values may be explained by the length of time that vegetation within the burn units has had to recover since the last burn.

Semi-automated delineation of vegetation stands could improve the efficiency with which City personnel are able to map vegetation stands across large extents and subsequently estimate bare, herbaceous, and shrub cover within the stands. The project evaluated multiple techniques for semi-automated delineation of vegetation stands. The extent to which derived polygons replicated the stand polygons field mapped by the City was assessed by comparing image-derived vegetation stand polygons to those mapped in the field by City personnel in April 2002. Overall, the field delineated boundaries generally were not accurately reproduced by automated techniques, as transitions between stands of vegetation with varying percentages of shrub, herb, and bare ground do not have distinct edges. Visual interpretation and "heads-up" digitizing on a digital image may be the most effective way to reduce the need for fieldwork, while maintaining the expert opinion of a biologist/analyst in the delineation of vegetation stands. Alternatively, the spatial units that are generated from image segmentation routines could serve as the basis for long term monitoring.

Results from this study indicate that image-based assessment of shrub, herbaceous, and bare soil cover may be sufficiently accurate to be adopted by the City as a method for regular monitoring of vegetation and habitat quality within the MSCP reserve. We provide specific recommendations for image acquisition and processing procedures which should enable the City to initiate a successful remote sensing-based mapping and monitoring program.

1.0 Introduction and Project Objectives

Management of natural lands and resources within the Multiple Species Conservation Program (MSCP) requires frequent assessment of vegetation and habitat condition, and changes in condition. Remotely sensed imagery has the potential to provide wall-to-wall coverage of habitat reserves and enables land managers to assess and document the condition of natural lands. Further, multitemporal remotely sensed imagery enables the detection of changes in land cover condition over time.

The percentages of shrub, herbaceous (herb), and bare ground (bare) cover within stands of natural vegetation in southern California may be an indicator of habitat quality. Remotely sensed imagery may be exploited to estimate the cover proportions of these general land cover types. The primary objective of this project was to assess the utility of airborne multispectral imagery for estimating shrub, herb, and bare cover within habitat reserves. This assessment was based on single date and multitemporal imagery, within which temporal differences in vegetation phenology were evaluated for discriminating vegetation cover types. Secondary objectives were to: 1) characterize the spectral signatures of dominant plant species and exotic plant species, 2) investigate correlations between post-fire stand age and image spectral/radiometric characteristics, and 3) assess the utility of imagery for semi-automated vegetation stand delineation.

2.0 Study Area and Data

The City of San Diego property within Marron Valley was the study site. Marron Valley is a small valley located between Otay Mountain and Tecate Mountain, along the U.S./Mexico border in southern San Diego County. The site is dominated by coastal sage scrub vegetation, with areas of southern mixed chaparral, chamise chaparral, and non-native grassland. The terrain within this 6.8 km by 3.5 km site is characterized as mountainous, with an elevation range of 143 m to 538 m and an average slope of 20 degrees.

On December 7, 1999 the City of San Diego (City) placed a conservation easement on this 2,600 acre property at Marron Valley (Story, 2000). In March, 2002 cattle were removed and grazing ceased on the property. Habitat with Marron Valley is expected to recover from grazing-related activities, and the property provided a good site for assessing the utility of image-based monitoring.

Airborne Data Acquisition and Registration (ADAR) 5500 imagery was acquired with 1 m spatial resolution at Marron Valley on 11 April 2002 and 24 August 2002 from a helicopter platform. The 24 August 2002 imagery was acquired using a frame center (FC) matching approach developed by San Diego State University (Appendix A), so that the multitemporal image sets could be precisely registered to each other. A diagram illustrating the concept of frame center matched image frames is shown in Figure 1. Using this approach, a global positioning system (GPS) incorporating frame center positions from the previous flight (April 2002) was utilized to guide the pilot down the previously flown flight path and trigger the

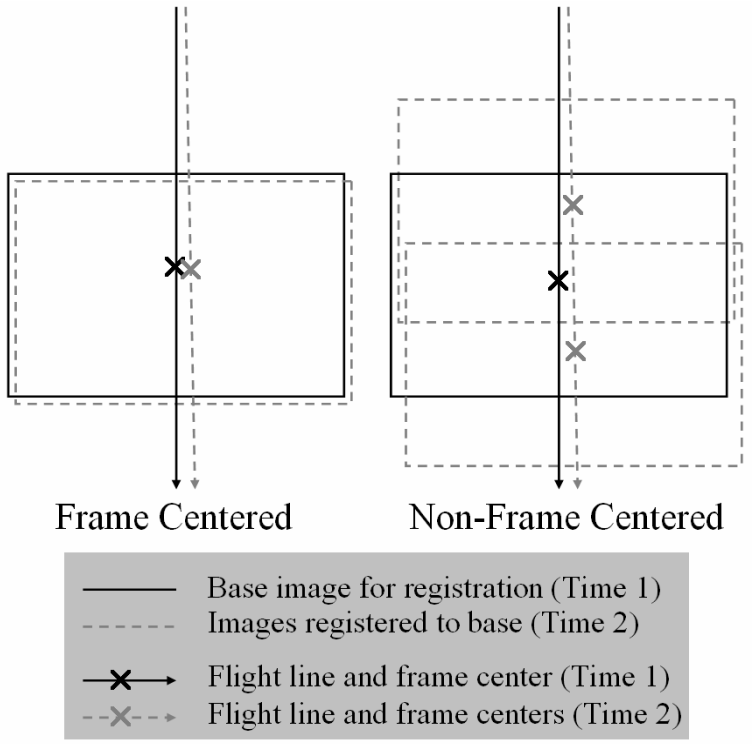

Figure 1. Diagram illustrating frame centered vs. non-frame centered image acquisition.

cameras at the same camera stations from which image frames were acquired in April. This approach to image acquisition replicates camera view and terrain distortions between multitemporal image frame pairs and enables precise registration between image frames, even in areas of high and variable terrain.

Field data were collected at by the City between 25 March and 28 March 2002. Fifty two polygons containing a range of vegetation community types and percent cover of shrub, herb, bare and were mapped for selected portions of the City property within Marron Valley (Figure 2). The following attributes were recorded for each polygon mapped: stand number, elevation (ft), slope (%), bearing (degrees), total vegetation cover (%), shrub cover (%), herb cover (%), and non-native cover (%), species cover (%), survey date, and survey personnel.

3.0 Methods

3.1 Image Acquisition and Preprocessing

ADAR 5500 imagery with 1 m resolution was initially acquired for the Marron Valley site on April 11, 2002. On August 24, 2002, FC matched image frames were again acquired at 1 m resolution using the GPS-based camera triggering system at each of the image stations previously visited on April 11, 2002. Following image acquisition, the blue (450-540 nm), green (520-600 nm), red (610-690 nm), and near-infrared (780-1000 nm) wavebands of the individual ADAR

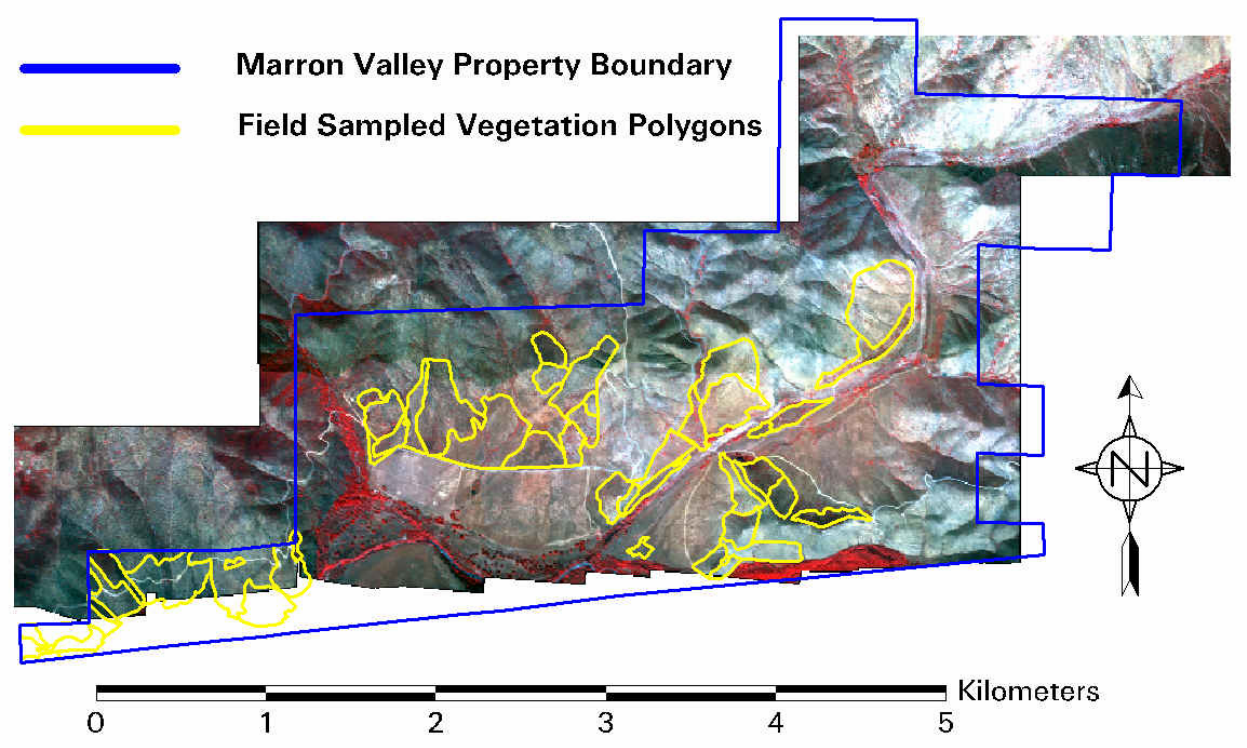

Figure 2. Field mapped polygons within the City property at Marron Valley. The background image is a mosaic of ADAR 5500 imagery acquired in April 2002 (display is near-infrared, red, and green wavebands in red, green, and blue color planes, respectively).

image frames were band-to-band registered and vignette corrected, as part of standard ADAR 5500 preprocessing. The ADAR frames were also corrected per-waveband for anisotropic reflectance effects, which cause variations in digital number (DN) values across image frames due to differences in sun-scene-sensor geometry. This correction process substantially reduced anisotropic variations in image brightness across and between ADAR image frames.

The individual FC matched images acquired in August using the GPS-based triggering system were registered to corresponding image frames acquired in April, on a per-frame basis. This was accomplished using automated ground control point (GCP) collection and second-order polynomial warping transformations in Digital Images Made Easy (DIME) software by Positive Systems, Inc. Between 150 and 400 well distributed GCPs were utilized to register each of the FC matched image frames.

The acquisition of FC matched image sets was successful and enabled precise registration between April and August ADAR image pairs. Flight altitude was monitored using the aircraft altimeter and altitudes were matched within 64 m on average (according to uncorrected GPS readings) (Table 1). Using non-differentially corrected, real-time GPS readings for flight line navigation and automatic camera triggering, the average error in replicating the horizontal position of camera stations was 43 m (Table 1). The maximum distance between corresponding camera stations was 174 m, while the minimum distance was 3 m. These measurements of camera station offsets were based upon non-differentially corrected GPS readings from the

ADAR 5500 system, which utilized a different GPS system than that used for navigation and camera triggering. The largest errors in replicating horizontal frame center positions were associated with aircraft deviations from the planned flight line and not with the GPS-based triggering.

Registration root mean square error (RMSE) values provide a measure of overall positional difference between two image data sets, and is computed using coordinates from corresponding ground feature test points and Equation 1.

$$\text{RMSE} = \sqrt{\frac{1}{n}\sum_{i=1}^{n}\Delta X_i^2 + \Delta Y_i^2} \quad (1)$$

Where:
n = the number of test points
i = test point (TP) number
ΔX_i = the X misregistration distance for TP_i
ΔY_i = the Y misregistration distance for TP_i

Registration RMSE values between the April and August ADAR image sets were generated independently using approximately 100 automatically derived check points per frame set. The average registration RMSE between the frame center matched image sets was 2.3 pixels (Table 1). The minimum and maximum RMSE values were 1.1 and 6.1 pixels, respectively.

Table 1. Image acquisition and registration summary statistics of frame center matched image pairs from Marron Valley.

Summary Measure	Altitude Offset (m)	Horizontal Offset (m)	RMSE (Pixels)
Mean	64	43	2.3
Standard Deviation	59	46	0.9
Minimum	0	3	1.1
Maximum	153	174	6.1

RMSE = root mean square error

Following image-to-image registration of the FC matched image pairs, each of the registered image pairs were combined to create a single eight-layer image frame. Overlapping portions of the individual image sets which had data from both the April and August acquisition were subset from the registered image pairs. These eight-layer subset images were then georeferenced and mosaicked using semi-automated image-to-image registration in DIME and the SANDAG 2000 CIR orthophotograph product as the registration base. The resulting mosaic provided a precisely registered, multitemporal image set containing data from the April and August acquisitions. The April and August image layers were then separated into two mosaics (Figure 3).

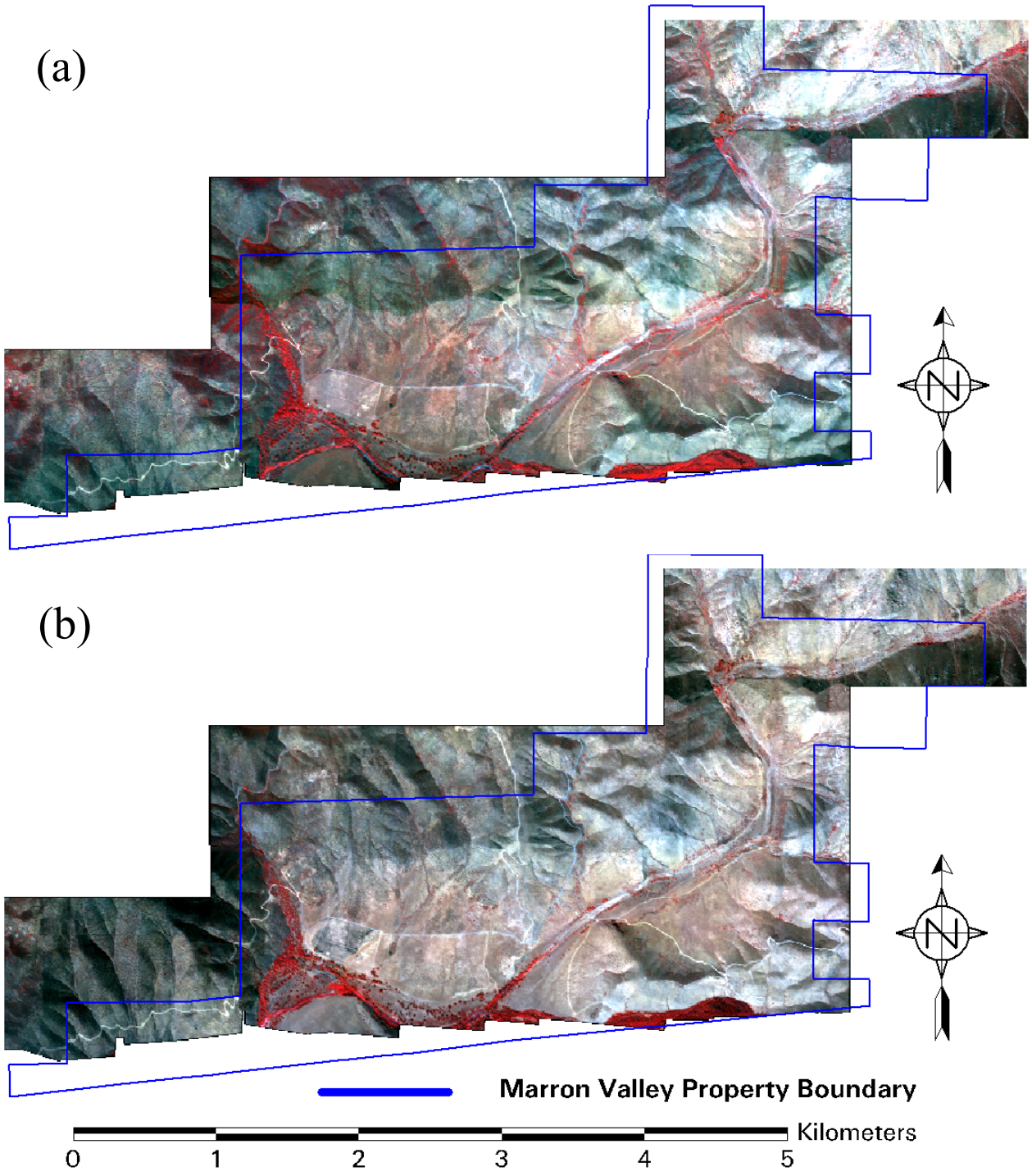

Figure 3. April (a) and August (b) ADAR 5500 mosaics from Marron Valley. Display is near-infrared, red, and green wavebands.

3.2 Image-Derived Estimates of Shrub, Herbaceous, and Bare Ground Cover

The project team sought to identify an efficient and objective procedure for image-based classification of land cover materials relating to habitat condition and quality that would be applicable to the entire MSCP and repeatable. Further, the team sought to identify an approach that would be minimally dependent upon the skill and experience of image analysts.

Multiple procedures were evaluated for classifying shrub, herb, and bare cover using single date and multidate ADAR 5500 imagery. These included: model-based classification of multidate image products, model-based classification of single date image products, unsupervised classification of multidate image products, and unsupervised classification of single date image products.

Model-based classification of single and multiple date ADAR imagery was performed using the Imagine Expert Classifier (Leica Geosystems, Inc.). This software provides a rule-based approach to multispectral image classification. Unsupervised image classifications with single and multiple date imagery were performed using the ISODATA spectral clustering algorithm available in Imagine. This algorithm iteratively clusters image data into a user specified number of spectral cluster classes, and the analyst then interprets each spectral cluster class to determine to which map class it corresponds. For each unsupervised image classification, 100 spectral cluster classes were output by the ISODATA algorithm and labeled by the analyst.

The normalized difference vegetation index (NDVI) spectral vegetation index is calculated using Equation 2 and has been shown to be related to plant leaf area, biomass, and absorbed photosynthetically active radiation (Myneni et al., 1995; Phinn et al., 1996; Phinn et al., 1999). The NDVI provides unique information about vegetation cover and yields standardized values between multitemporal image acquisitions. In addition, the NDVI normalizes imagery for brightness variations associated with terrain aspect and terrain shadowing. For these reasons, the NDVI may provide an effective mean of monitoring changes in vegetation cover and condition. The NDVI was utilized in each of the image classification processes.

$$\text{NDVI} = (\text{near-infrared} - \text{red}) / (\text{near-infrared} + \text{red}) \quad (2)$$

For the unsupervised image classifications, the NDVI was added as an additional image layer, and unsupervised clustering was performed using the spectral waveband data and the NDVI. Expert Classifier models utilized in this study incorporated April and August NDVI values, NDVI multitemporal difference values, red waveband texture, and values from a soil index that is created by dividing calculating a normalized difference between red waveband and blue waveband values (Equation 3). The soil index exploits characteristic differences in the red and blue reflectance of soil. The red waveband texture values were created for each pixel by computing the standard deviation of pixel values within a 3x3 pixel window around each pixel. The red waveband texture values provide an indication of the heterogeneity within the landscape adjacent to each pixel, and are useful for discriminating shrub from herb cover. A list of each input image layer per classification method is given in Table 2.

$$\text{Soil Index} = (\text{red} - \text{blue}) / (\text{red} + \text{blue}) \quad (3)$$

Table 2. Image inputs for multiple image classification approaches.

Input Layers	April Unsup.	August Unsup.	Multidate Unsup.	Multidate Exp. Classif.	August Exp. Classif.
April Red, NIR Bands	xxx		xxx		
April NDVI	xxx		xxx	xxx	
August Red, NIR Bands		xxx	xxx		
August NDVI		xxx	xxx	xxx	xxx
Apr.–Aug. NDVI Diff.				xxx	
April Red Band Texture				xxx	
August Red Band Texture					xxx
April Soil Index				xxx	
August Soil Index					xxx

3.2.1 Calibration of Image-Derived Estimates of Percent Cover

A sample set of the field data collected by the City was utilized as reference data to calibrate image classifications of shrub, herb, and bare. Operational monitoring of habitat quality will also require some field data collection for calibration or training of image classifications.

Ten field mapped polygons and corresponding values of percent cover were utilized for calibration. These polygons were identified by the City during the field sampling as stand numbers 12, 19, 23, 28, 30, 32, 36, 41, 46, and 52. The process was iterative and included the following steps: 1) an image classification was generated, 2) the percent cover of shrub, herb, and bare per sample polygon was summarized, 3) the cover percentages were compared to the reference data using scatterplots and RMSE values between the image-derived and reference cover percentages, 4) the classification was adjusted, and 5) percentages were re-compared to the reference data. This process continued until systematic differences between the image-classification derived percentages and reference percentages were minimized and only non-systematic differences remained. These non-systematic differences represented errors that could not be resolved through refinement in the image classification process.

Unsupervised image classifications were calibrated by changing the map class (shrub, herb, or bare) into which some of the spectral cluster classes likely containing mixed land cover were assigned. For the single and multiple date unsupervised classifications, approximately 15 of the 100 spectral cluster classes were edited and labeled with a different map class during the calibration process. Model-based classifications were adjusted by changing the model parameters. The final Expert Classifier models for multidate and single date classifications are given in Figure 4 and Figure 5, respectively. A full description of the processes operating within the Expert Classifier models is given in Appendix B.

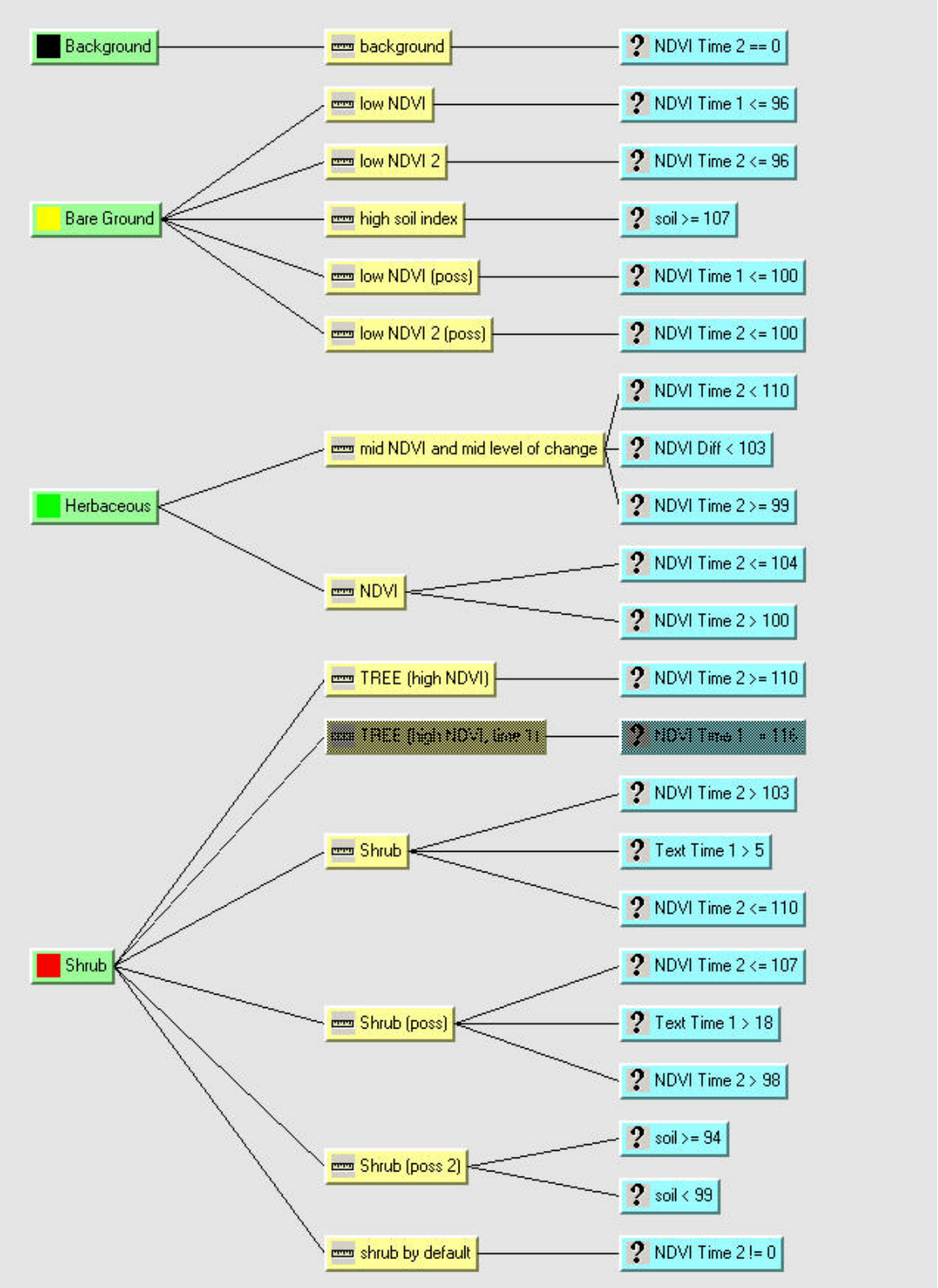

Figure 4. April and August multidate Expert Classifier model.

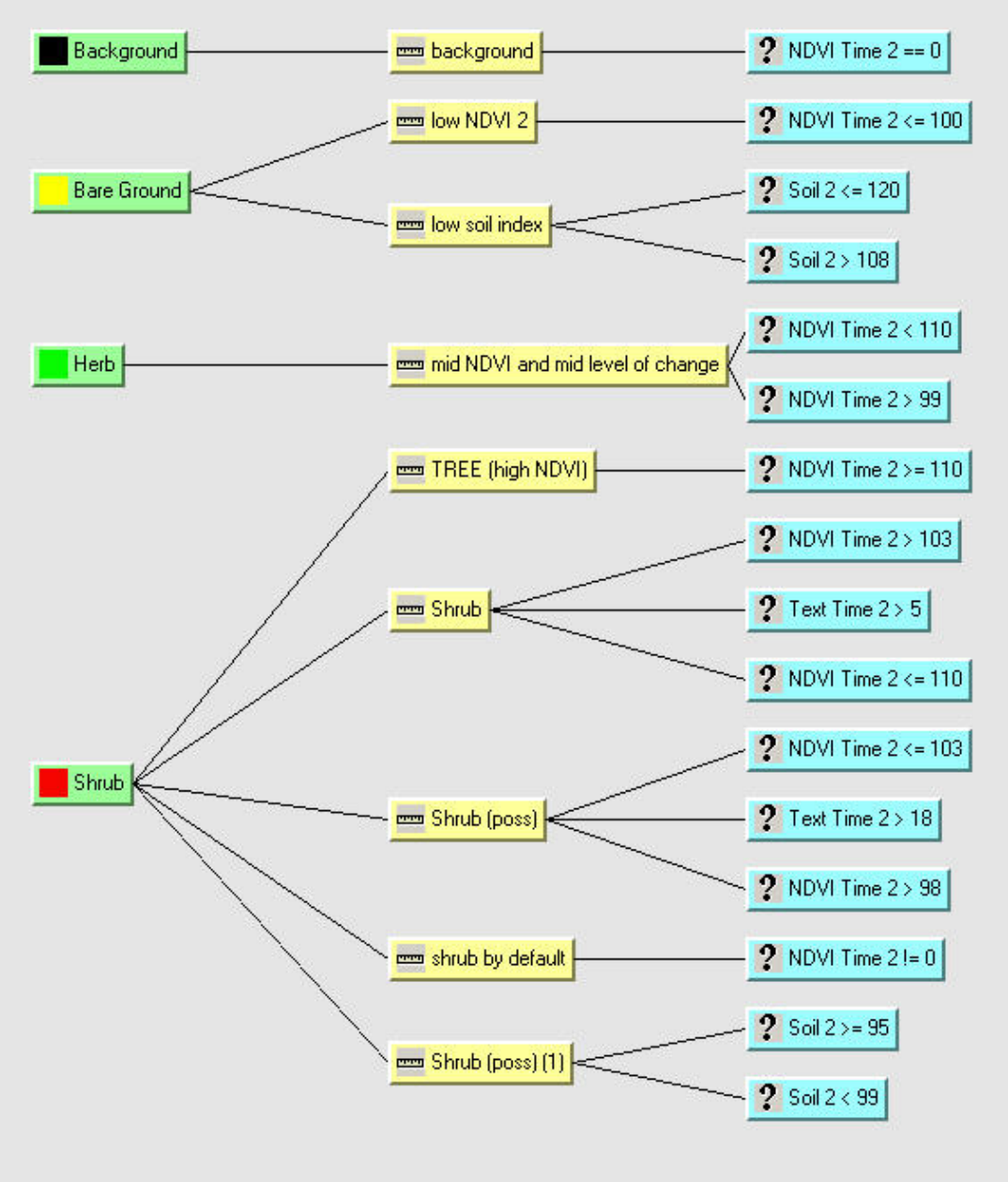

Figure 5. August Expert Classifier model.

3.2.2 Validation of Image-Derived Estimates of Percent Cover

Of the 52 polygons field mapped by the City, seven were not completely covered within the ADAR mosaics and ten were used for calibration. The percent cover of shrub, herb, and bare covers derived through image classification was validated using the remaining 35 polygons. Derived cover percentages were compared to the reference cover percentages on a per-polygon basis. Scatterplots and values of RMSE were generated to summarize the error of image-derived cover percentages, relative to those obtained through field mapping by the City. The RMSE for shrub, herbaceous, and bare cover was calculated using Equation 4. Overall RMSE for all cover types was also calculated using Equation 4.

$$\text{RMSE} = \sqrt{\frac{1}{n}\sum_{i=1}^{n}(I_i - F_i)^2} \quad (4)$$

Where:
n = the number of polygons
i = polygon number
I_i = image-derived cover percentage
F_i = field estimated cover percentage

3.2.3 Optimization of Image Classifications

The validation process described above identified the magnitude of error that was likely to be present within entire image classification products that were calibrated using a limited number of field mapped reference samples. We also sought to identify the overall information content within airborne multispectral imagery by identifying the error magnitudes between semi-automated image classification products and field mapped reference polygons when all information was available for calibrating the image classifications.

Optimization of the image classification products was performed by using all field mapped reference information that was available. Unsupervised and model-based image classifications were fine-tuned so that the error between image-derived and reference values of shrub, herb, and bare cover were minimized for all 45 polygons utilized in this study. Cover proportions within final optimized image classification products were then compared to the reference proportions using scatterplots and RMSE measures, and validation was performed using reference data from all 45 polygons.

3.3 Spectral Signatures of Dominant and Exotic Species

Spectral signatures were compiled from areas field mapped by the City as having high percentages of individual native and exotic species. The goal was to identify any unique spectral characteristics which may be utilized to detect and classify these plant species within multispectral imagery. Within the vegetation stands field mapped by the City, only four stands contained greater than 50% cover of a single species. Therefore, a threshold of 33.33% cover of an individual species was selected as the minimum cover at which a single species was considered the predominant cover within a stand.

Only 12 stands contained greater than 33.33% cover of a single plant species. Of those, three stands were not imaged during the April and August image acquisitions and could not be used in the analysis. Of the remaining nine stands, seven were dominated by the non-native species *Erodium botrys*, one was dominated by the native species *Adenostoma fasciculatum*, and one was dominated by the native plant species *Selaginella bigelovii*. Spectral signatures were extracted from the image data for each of the nine stands dominated by the above species.

3.4 Effect of Fire History on Image Spectral/Radiometric Characteristics

The effect of fire on chaparral and coastal sage scrub (CSS) landscapes is well documented (Keeley, 2000; O'Leary, 1990). While fire is a natural component of these community types, it has the potential to alter landscapes. Depending upon fire intensity and frequency, vegetation within an affected area can type-convert and may take many decades to return to its original state. Even without type conversion, vegetation recovery following the burn takes years to decades.

The recovery of vegetation following a fire is important to monitor, as it is directly related to the recovery of habitat within affected areas. The project assessed whether or not fire affected areas have characteristically different spectral reflectance than non-fire affected areas and if airborne multispectral imagery could provide information on the status of fire recovery.

The immediate effect of fire on CSS landscapes is removal of vegetation cover, fire scarring, and deposition of ash onto the soil. During the first winter season, ash deposits are washed away leaving sparsely vegetated landscapes with high soil cover. This high soil cover results in greater overall surface brightness. As vegetation within affected areas recovers, soil exposure decreases and vegetation cover increases, initially with dominance of herbaceous plants and then reestablishment of shrubs. The vegetation recovery decreases the overall surface brightness.

Principal components analysis (PCA) is a decorrelation and data reduction technique which may be applied to remotely sensed imagery to remove the correlation between multispectral data and create new, uncorrelated image layers. When applied to color infrared imagery, values of the first principal component layer (PC1) generally correspond to overall image brightness within the original multispectral image set.

The project investigated whether or not there was a relationship between overall image brightness and the number of years since the last fire, within areas in Marron Valley known to have burned within the last 35 years. If relationships exist between these variables, then measures of overall image brightness may provide information on the post-fire recovery of CSS and chaparral vegetation. Single date and multidate ADAR mosaics were subjected to principal components analysis, and PC1 image layers were derived from the April ADAR mosaic, the August ADAR mosaic, and the April and August multidate ADAR mosaic. The overall image brightness (as indicated by average PC1 values) was summarized for each burn unit. PC1 values of overall brightness were plotted against the number of years since last fire within for each burn unit. The scatterplots were analyzed and apparent relationships summarized. For the analysis, PC1 values were scaled to range from 0-255.

3.5 Semi-Automated Delineation of Vegetation Stands

Semi-automated delineation of vegetation stands could improve the efficiency with which City personnel are able to map vegetation stands across large extents and subsequently estimate bare, herbaceous, and shrub cover within the stands. As part of the Marron Valley habitat monitoring project, SDSU personnel evaluated techniques for semi-automated delineation of vegetation stands using multiple image processing techniques. The extent to which semi-automated delineation of vegetation stands boundaries replicated the stand polygons field mapped by the City was assessed by comparing image-derived vegetation stand polygons to those mapped in the field by City personnel in April 2002.

City personnel delineated vegetation stand polygons in the field by interpreting color-infrared orthophotographic images in conjunction with in-situ observation. Natural breaks in vegetation cover were identified and delineated onto hardcopy plots of the color-infrared imagery. These polygons were later digitized and coded into a geographic information system (GIS). Semi-automated techniques of stand delineation from imagery may reduce the time and costs, relative to the field-based methods used by the City in April 2002.

Image segmentation refers to image processing techniques for generating polygons of homogenous cover types from image data. Segmentation routines extract regions of coherent color and often texture (spatial variations in image brightness). Three different segmentation procedures were undertaken. These are listed below in order of automation, with the least automated first.

1. **Region Grow** is a tool that groups spectrally similar contiguous pixels into polygons. The region grow polygons were initiated from a single seed pixel within the field delineated polygons to determine whether the region grown areas match the areas delineated in the field. The region grow boundaries were generalized to smooth the pixel-induced shapes.
   This manually guided method should indicate whether the polygons are spectral distinct, this is required to enable the following remotely sensed procedures to produce any useful classification or segmentation results.
2. **Feature Analyst** uses spectral and spatial characteristics to classify imagery. The software is trained iteratively until the desired output is created. The training process can be very time consuming and may produce image-specific results.
3. **Unsupervised Classification** is a fully automated approach that groups the image data into a specified number of spectral classes. More classes are chosen than are required so that users can group similar classes. This method relies on the spectral characteristics of the cover-types. Post-classification procedures are also used to refine the classification and aggregate smaller polygons.

Further discussion of the semi-automated delineation of vegetation stands using segmentation techniques is given in Appendix C.

4.0 Results

4.1 Image-Derived Estimates of Shrub, Herbaceous, and Bare Ground Cover

The final image classification products are illustrated in Appendix D for model-based and unsupervised image classifications. Scatterplots of field estimated and image-derived cover percentages per polygon are graphed in Appendix E. The scatterplots enable review of systematic over or underestimation of cover, and the overall random variability between field estimated and image-derived cover estimates. Scatterplots are given for the calibrated sample set (10 polygons), the validation set (35 polygons) for calibrated classifications, the optimized full set (45 polygons), and the effect of optimization on the 10 polygon originally used for calibration.

RMSE between image-derived estimates of shrub, herb, and bare cover proportions and those field estimated by the City is summarized in Table 3 and Table 4 for calibrated image classifications and optimized image classifications, respectively. In each table, RMSE values are given individually for shrub, herb, and bare cover types and for the overall image classification accuracy. For the August unsupervised classification and the August Expert Classifier classification, the image classifications were not modified between the calibrated and the optimized products. However, RMSE values for calibrated and optimized products were calculated differently. Calibrated image classifications were validated using the 35 polygons not utilized during the calibration stage. This provides an independent assessment of calibrated image classification accuracy, and gives an estimate of likely errors that would be obtained when image classification is performed operationally using limited areas for calibration. Optimized classifications were validated using all 45 polygons, so that the potential accuracy that may be derived through image classification given all available information was assessed using all reference data available.

Table 3. RMSE value for shrub, herbaceous, and bare cover proportions derived from calibrated image classifications.

Classification Method	Shrub Cover RMSE	Herb Cover RMSE	Bare Cover RMSE	Overall RMSE
April Unsup	17.4	21.5	21.4	20.2
Aug. Unsup.	25.3	23.7	24.1	24.4
Multidate Unsup.	15.3	18.3	25.0	19.9
Aug. Exp. Classif.	11.4	18.5	24.4	18.8
Multidate Exp. Classif.	11.4	20.3	26.2	20.2

Measures of overall classification accuracy indicate that image classifications and derived estimates of shrub, herb, and bare cover have an overall RMSE of approximately 20%. Therefore, 68% of all cover estimates vary by less than 20% cover, relative to the field-estimated shrub, herb, and bare cover. In general, there were not large differences in overall classification

Table 4. RMSE value for shrub, herbaceous, and bare cover proportions derived from optimized image classifications.

Classification Method	Shrub Cover RMSE	Herb Cover RMSE	Bare Cover RMSE	Overall RMSE
April Unsup	25.4	18.4	26.4	23.4
Aug. Unsup.	24.1	22.9	22.5	23.2
Multidate Unsup.	15.5	14.6	21.8	17.3
Aug. Exp. Classif.	11.7	17.7	23.3	17.6
Multidate Exp. Classif.	11.7	19.1	25.1	18.6

accuracy between the calibrated image classifications and the optimized image classifications. The optimized multidate unsupervised image classification yielded the highest overall classification accuracy, with an overall RMSE of 17.3%. However, the August Expert Classifier classification (calibrated and optimized) yielded similar results, with an overall RMSE of 17.6% (when validated using all 45 polygons).

Estimates of shrub cover derived through classification with the Expert Classifier yielded the lowest RMSE (~11%). This is largely attributed to the primary use of NDVI to classify shrubs in the Expert Classifier models. NDVI normalizes brightness differences caused by terrain shadow and provides a clearer representation of the actual distribution of shrubs. Unsupervised classifications which utilized brightness values from the red and near-infrared spectral bands, in addition to the NDVI, generally overestimated shrub cover in areas of terrain shadow. This results because shrubs and terrain shadows are dark in the red waveband.

The largest errors in classifying herbaceous cover were due to under-classification of herb. This points to the problem of discriminating herb from shrub in spring (April) and herb from bare ground in the summer (August). However, systematic under-estimation was largely minimized, and much of the error is random. Therefore, further of review of the imagery and refinement of classification parameters is not likely to substantially lower classification error.

Bare ground cover was generally underestimated in the April unsupervised classifications and overestimated in the multidate Expert Classifier classifications. No systematic errors in the classification of bare ground are present in the other classification products. The underestimation of bare ground in the April unsupervised classifications is attributed to the over-classification of shrub cover in these classifications. The overestimation of bare ground within the multidate Expert Classifier classifications indicates that further modification of model parameters is required to reduce the systematic error.

4.2 Spectral Signatures of Dominant and Exotic Species

The analysis of spectral signatures was limited due to the mixture of cover types present in polygons minimally dominated by greater than 33% cover of a single plant species. In addition, only three species were found to have dominant cover percentage greater than 33% within the field mapped polygons. The vegetation stands from which spectral signatures were derived are illustrated in Figure 6. Stand numbers for each polygon are indicated in Figure 6. The mean spectral signatures (in digital number units) for each stand in April and August are graphed in Figure 7. Chart legends in Figure 7 indicate the species abbreviation and the stand number from which each spectral signature was extracted.

Spectral variability was generally greater between signatures in April. In August, vegetation within the stands was dryer and there was less spectral variability. However, the *Selaginella bigelovii* and most of the *Erodium botrys* dominated stands exhibited little change in spectral response between April and August. The largest changes in spectral response between April and August were associated with differences in illumination and terrain shadowing (stands 11 and 31).

From Figure 7, it appears that the spectral signature from the single stand dominated by *Selaginella bigelovii* is not spectrally separable from the signatures of stands dominated by *Erodium botrys*. The spectral signature from the single stand dominated by *Adenostoma fasciculatum* appear to be spectrally separable from spectral signatures of the other two vegetation types. However, this vegetation stand (# 11) is located within a terrain shaded area. The low spectral-radiometric values, relative to other signatures, may only result from the terrain shadowing. Therefore, there is not sufficient information to draw significant conclusions.

Future analysis of vegetation spectral characteristics should include ground-based collection of spectra and detailed mapping of the locations of specific plants of interest within acquired airborne imagery. This would enable more detailed investigation of the spectral characteristics of native and non-native plants within *in-situ* and airborne spectral-radiometric measurements.

4.3 Effect of Fire History on Image Spectral/Radiometric Characteristics

Scatterplots with average PC1 values per burn unit plotted against the number of years since last burn per unit are given in Figure 8. The strongest relationship between overall image brightness (as indicated by PC1 values) and number of years since last burn was found within the April ADAR data set. The coefficient of determination (R^2) value obtained from a simple linear regression between average PC1 values per burn unit and the number of years since last burn per unit was 0.4352. While there are only eight samples in this analysis, this result suggests that over 40% of the variation in PC1 values may be explained by the length of time that vegetation within the burn units has had to recover since the last burn. Burn units and the number of years since burn are displayed with the April PC1 and April color infrared composite in Figure 9.

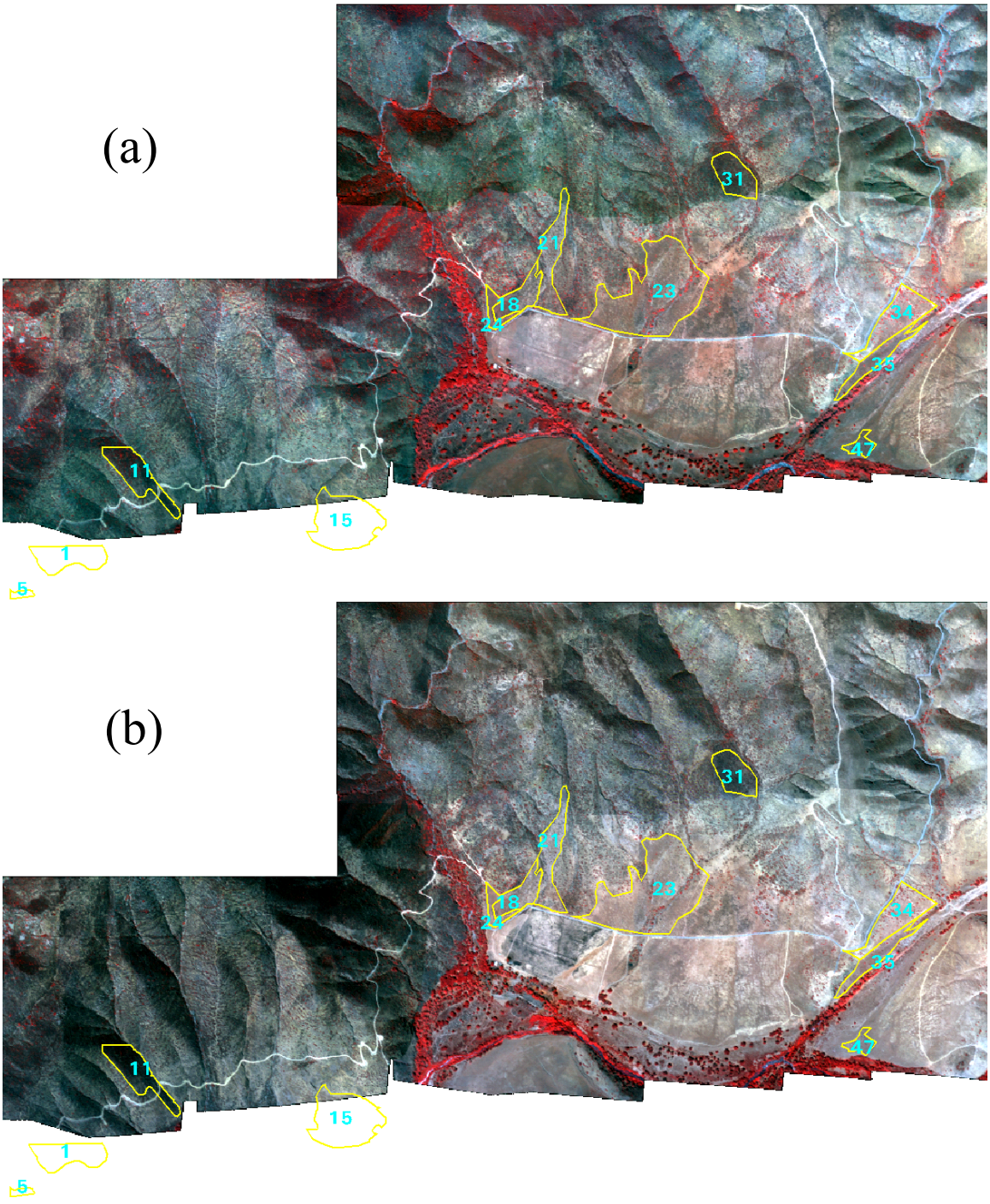

Figure 6. Polygons with dominant cover (> 33%) of a single species overlain on a portion of the (a) April ADAR mosaic and (b) August ADAR mosaic. Numbers indicate stand number.

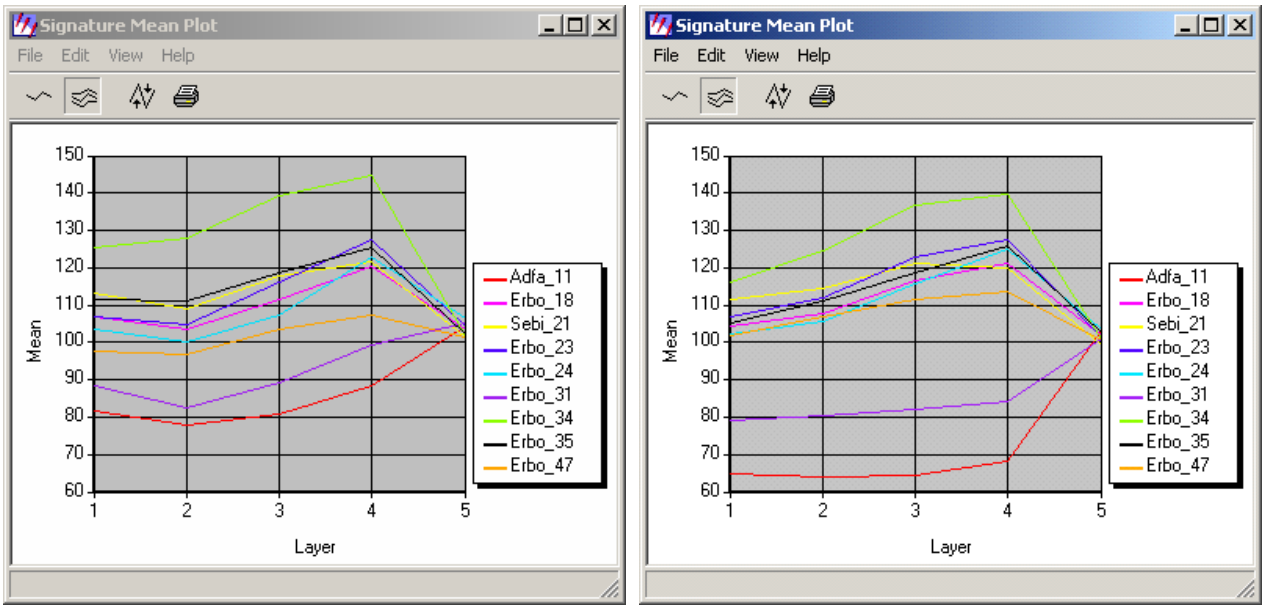

(a) April Signatures (a) August Signatures

Figure 7. Spectral signature plots from (a) April and (b) August image mosaics. Adfa = Adenostoma fasciculatum, Erbo = Erodium botrys, Sebi = Selaginella bigelovii. Layers 1-4 correspond to blue, green, red, and near-infrared wavebands, respectively. Layer 5 corresponds to the normalized difference vegetation index (NDVI). The NDVI range is reduced relative to that of the multispectral wavebands, as a result of the processing applied to create that layer. Spectral-radiometric units (y-axis) are digital numbers.

August PC1 and multidate (April and August) PC1 exhibited lower correlation with years since last burn, with R^2 values of 0.3115 and 0.3828, respectively. The lower correlation exhibited by the August PC1 data set (and multidate because August is included) is mostly attributed to illumination differences upon terrain slopes within the scene, relative to the April data set. Burn units 22 and 24 (label indicates years since last burn) show a substantially lower August PC1 values as a result of increased terrain shadowing within theses areas (Figure 10). Similarly, many slopes within the northern portion of burn unit 7 exhibit decreased PC1 values in the August PC1 image, resulting in lower correlation (Figure 10). In addition to illumination and shadowing differences, lower correlation values may also be attributed to decreases in shrub leaf area and herbaceous cover between April and August. However, this effect appears negligible.

(a)

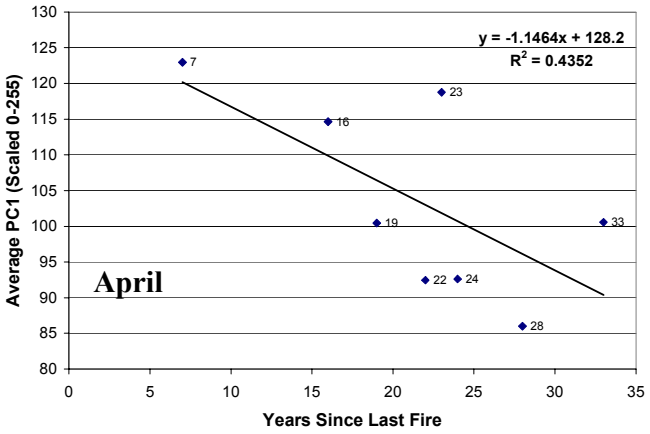

(b)

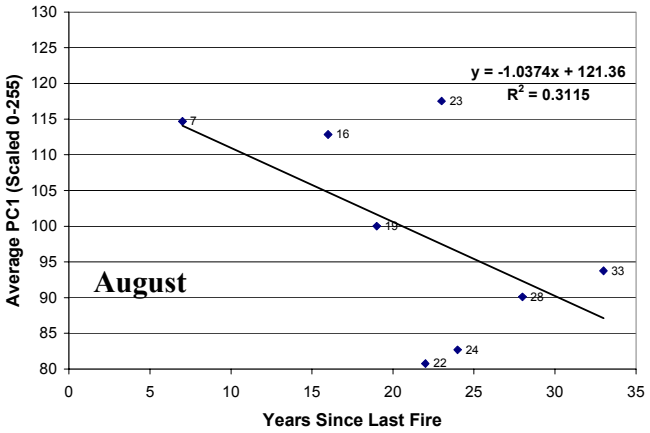

(c)

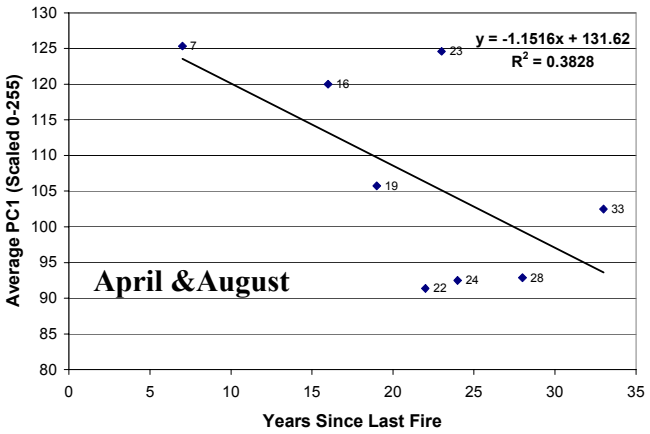

Figure 8. Scatterplots illustrating the relationship between years since last burn and overall image brightness as quantified by average first principal component values (per burn unit) derived from three image datasets: (a) April 2002 ADAR image mosaic, (b) August 2002 ADAR image mosaic, and (c) April and August multidate ADAR image mosaic. Simple linear regression equations and least squares lines are given on the scatterplots. Data point labels indicate the number of years since last burn and correspond to polygon labels in Figure 9 and Figure 10.

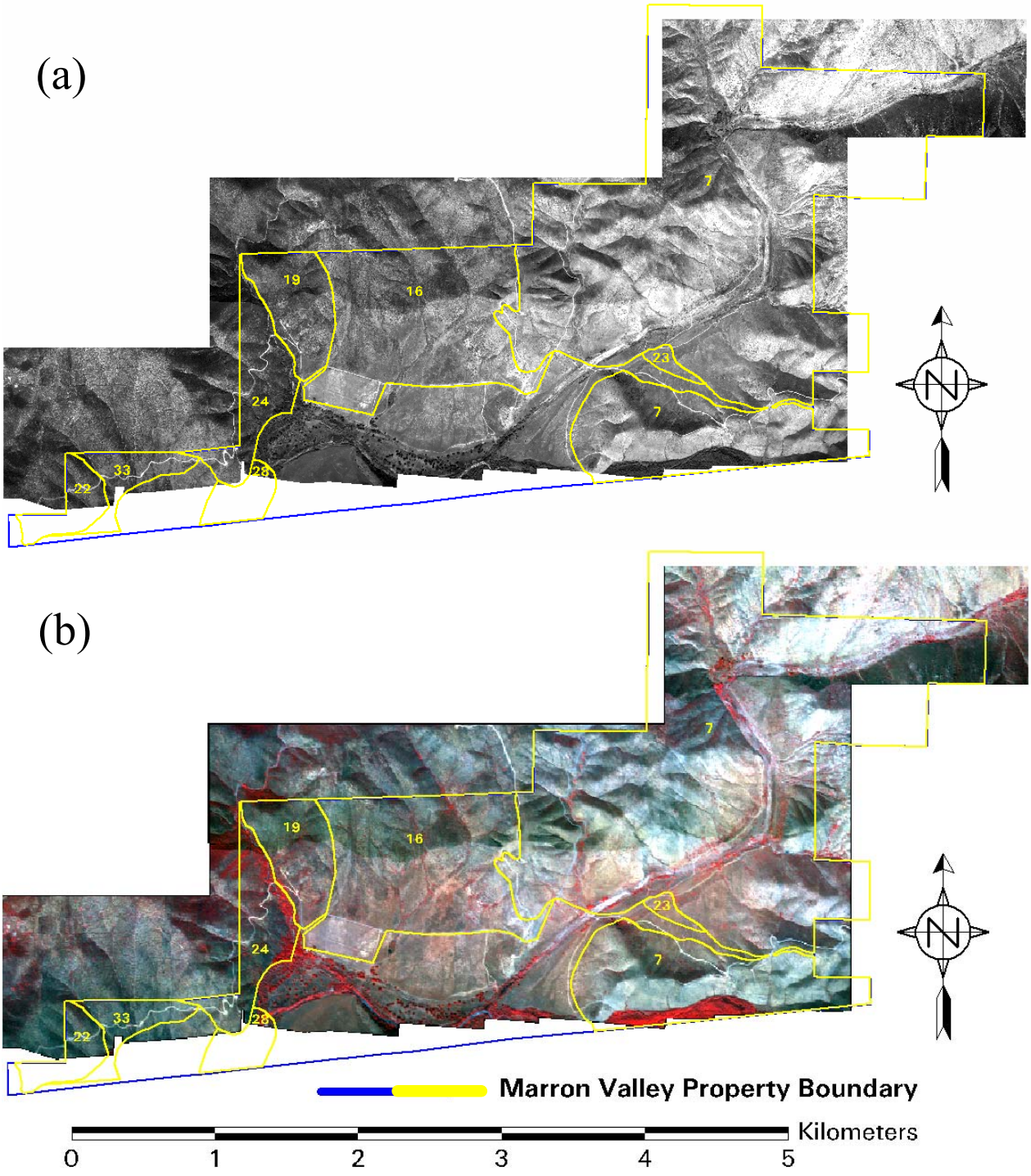

Figure 9. Burn units labeled with the number of years since last burn and displayed on (a) April PC1 image and (b) April multispectral image (display is color infrared).

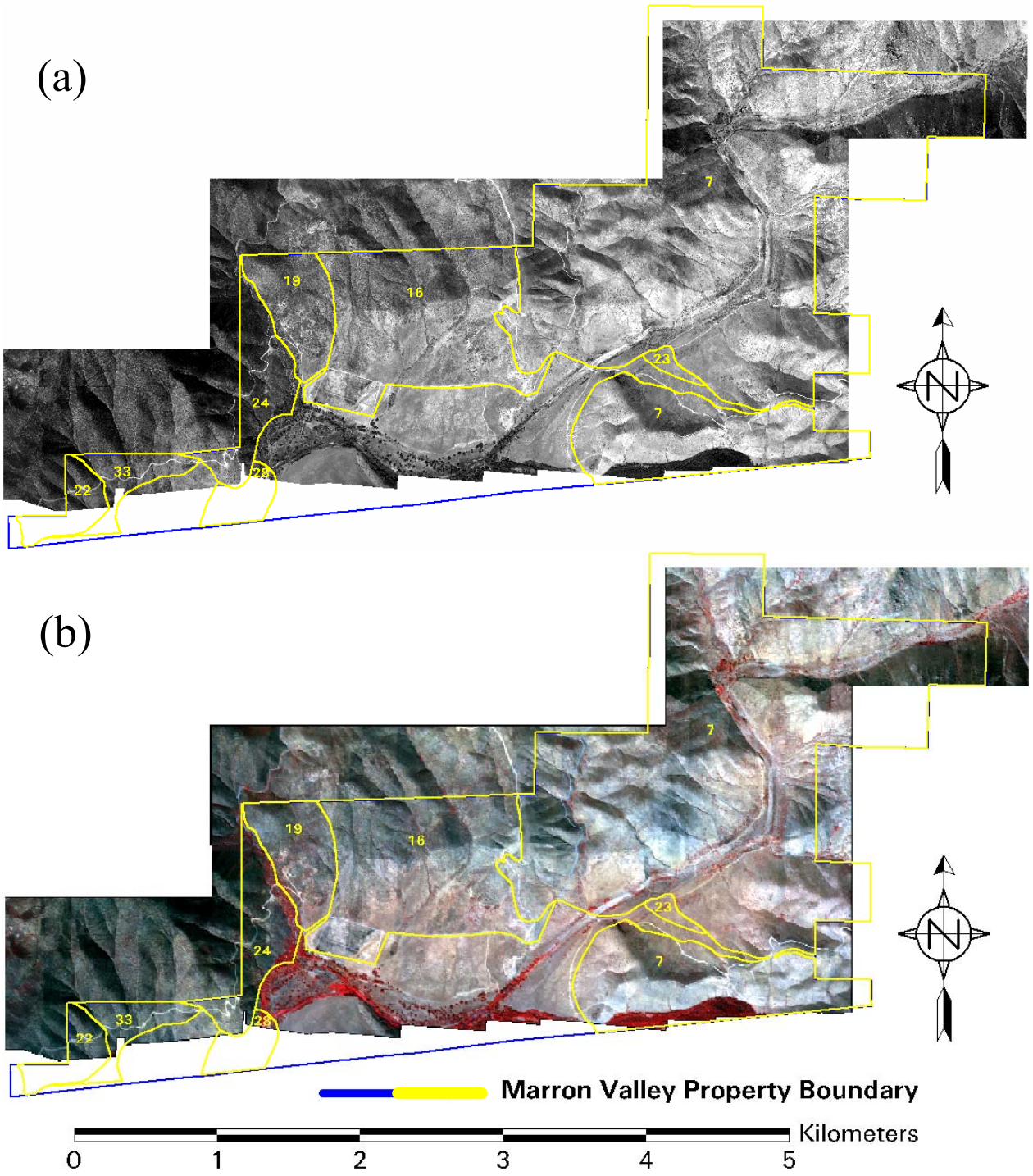

Figure 10. Burn units labeled with the number of years since last burn and displayed on (a) August PC1 image and (b) August multispectral image (display is color infrared).

4.4 Semi-Automated Delineation of Vegetation Stands

General results from the analysis of semi-automated delineation of vegetation stands are presented here. Detailed results and graphics from the analysis are given in Appendix C. From the imagery it is relatively easy to understand why the boundaries delineated in the field by City personnel were positioned where they were. However, some of the boundaries have been located in transitional areas containing multiple vegetation types rather than restricted to solely delineating a specific cover-type. This caused difficulties when trying to use the automated approaches to replicate these boundaries. Most polygons do not contain homogenous cover types, which was also problematic for the spectral approaches.

Region Grow: The generalized polygons provided similar extents to the field derived boundaries. However, the region grow operation is restricted in growth where there are spectrally different vegetation types. This makes the selection of the initial seed pixel important.

Feature Analyst: The software was trained extensively on the field derived polygons which was a time-intensive routine. The generated polygons matched the field derived polygons reasonably well for the more homogenous cover-types. The training process most likely was over-fit to the data and therefore, may only be applicable to this specific image-set. Analysis in other areas will likely require similar iterative training.

Unsupervised Classification: This process generally over-segmented the polygons. However, some user-input to regroup similar vegetation cover-types could produce better results. The more homogenous cover-types were more accurately delineated.

Overall, the field delineated boundaries generally were not accurately reproduced by automated techniques. The spectral characteristics of the vegetation enable semi-automated techniques to delineated boundaries of homogeneous cover types. The success of these techniques is limited in areas of heterogeneous vegetation cover. The feature analyst routine provided the most accurate delineation based on the field data, but is time-intensive and likely to be dataset specific. The unsupervised classification routine may be the most feasible operationally, as it is can be easily reproduced and is time-effective. However, it may produce more polygons than generated in the field.

While the polygons generated through semi-automated stand delineation techniques did not accurately match field delineated polygons, semi-automated routines do generate polygons of relatively homogeneous land cover units. City personnel should review the characteristics of the units generated through image segmentation routines and determine if these types of spatial units are appropriate for long term monitoring. If so, polygonal units generated through semi-automated segmentation of image data could be utilized for long term monitoring of habitat quality.

5.0 Conclusions

Model-based classification approaches such as that of the Expert Classifier utilizing NDVI and other data layers derived from single date, late summer imagery is expected to yield the most efficient, objective, and accurate classification of shrub, herb, and bare cover within San Diego County habitat reserves. In late summer (after mid-July), herbaceous vegetation has scenensed and is generally separable from shrubs and bare ground in multispectral imagery. In addition, the solar elevation is high at mid-day during this time of year, and imagery acquired at mid-day will have minimal terrain shadowing present. Use of the NDVI within model-based classifications is advantageous as the NDVI largely normalizes terrain shadows present in the imagery, and provides a clearer representation of the actual distribution of shrubs.

Application of model-based classifications to multitemporal imagery will enable quantification of cover proportions for each date of image acquisition, and quantification of changes in estimated cover proportions between dates. A single model with a fixed set of parameters may be utilized to classify cover proportions, if the multitemporal imagery are radiometrically normalized (so that index values are comparable) and if image acquisition is successfully controlled (so that illumination and terrain shadowing is not substantially different). If these conditions are not met, then refinement of models for each multitemporal image set may be required. Recommendations for image acquisition and processing are provided in the next section.

The analysis of spectral signatures was limited due to the mixture of cover types present in polygons minimally dominated by greater than 33% cover of a single plant species. From the analysis, it appears that the spectral signature from the single stand dominated by *Selaginella bigelovii* is not spectrally separable from the signatures of stands dominated by *Erodium botrys*. However, no significant conclusions may be drawn from the analysis of stand-based spectral signatures. Future analysis of vegetation spectral characteristics should include ground-based collection of spectra and detailed mapping of the locations of specific plants of interest within acquired airborne imagery.

The first principal component layer derived through principal components analysis with ADAR 5500 multispectral imagery exhibited inverse relationships with the number of years since last fire (R^2 values ranged from 0.31-0.44). The PC1 layer from April exhibited the strongest relationship, with an R^2 value of 0.4352. These results suggest that overall image brightness (as indicated by the PC1) may provide information of the recovery of vegetation from fire in CSS and chaparral landscapes. PC1 values are affected by terrain shadowing. Therefore, imagery should be acquired when the solar elevation (angle of the sun above the horizon) is high in order to minimize terrain shadowing.

Semi-automated delineation of vegetation stands may not be practical in CSS landscapes, as transitions between stands of vegetation with varying percentages of shrub, herb, and bare ground do not have distinct edges. As a result, vegetation stand boundaries derived through semi-automated delineation generally do not correspond well to those field mapped by biologists. Visual interpretation and "heads-up" digitizing on a digital image may be the most effective way to reduce the need for fieldwork, while maintaining the expert opinion of a

biologist/analyst in the delineation of vegetation stands. Alternatively, the spatial units that are generated from image segmentation routines could serve as the basis for long term monitoring.

6.0 Recommendations for Image-Based Assessment of Habitat Quality

The City anticipates using a multiple phase approach to accomplish broad area monitoring of habitat quality across the MSCP with minimal cost and resource allocation. This includes: 1) regular acquisition of high spatial resolution multispectral imagery, 2) change detection analysis to identify areas where habitat quality may be changing, 3) quantification of land cover (shrub, herbaceous, and bare) proportions within change areas, and 4) characterization of the type of change occurring within each change unit. Likely changes include: invasion of non-native plant species, fire, agriculture, illegal grading, and other disturbances which degrade native vegetation and habitat quality. We recommend the following procedures for image-based assessment of habitat quality.

6.1 Image Acquisition

Acquisition of imagery in late July or August may be optimal, as most herbaceous vegetation has scenensed and is spectrally separable from shrubs. The solar elevation is high at this time of the year. Imagery should be acquired near solar-noon, to achieve the highest solar elevation, and reduce terrain shadowing within the imagery.

Imagery should be acquired with matched frame centers, so that geometric characteristics of multitemporal image frames are consistent and the image frames may be registered with high precision.

6.2 Image Preprocessing

Radiometric and geometric correction of multidate imagery is essential for effective change detection and analysis of multitemporal imagery. Radiometric correction includes adjusting for changes in brightness across and between image frames which results from anisotropic reflectance, and normalization of image brightness values between dates. Geometric correction entails registering multitemporal images so that features overlap precisely between multitemporal image sets.

Correction of anisotropic reflectance within and between image frames may be accomplished using procedures outlined in Coulter et al., 2003. This correction is applied to raw image frames prior to any other preprocessing.

Geometric registration of multitemporal imagery may be performed using the procedures outline in section 3.1. For increased efficiency, baseline imagery acquired on the first year may be registered to a digital orthophotographic base image (such as the SANDAG 2000 color-infrared product) and mosaicked. Then newly acquired multitemporal image sets may be registered to the baseline image mosaic. The DIME software utilized for this study provides an efficient means for georeferencing and mosaicking image frames to a base image.

Following anisotropic correction of the imagery and creation of multitemporal image mosaics, radiometric normalization of image brightness values between dates should be performed. The most robust approach would be to calibrate each image set to values of reflectance. This would require that features with known reflectance be imaged during each acquisition. Linear relationships between recorded image brightness and values of reflectance could then be generated and used to transform image brightness values to values of reflectance. If normalizing to values of reflectance is not practical, then relative radiometric normalization may be performed, where image brightness values from multitemporal acquisitions are matched to those of the base image. Regardless of the approach used, the importance of radiometric normalization is that brightness values and values from derived image indices are consistent and meaningful between multitemporal image sets.

6.3 Image-Based Change Detection

The simplest and most efficient approach to image-based change detection analysis is image differencing, where brightness values from multitemporal image sets are subtracted from each other. Change areas exhibit the highest magnitude differences. A binary image indicating "change" or "no change" may be created by classifying change as those areas with difference values at or above a threshold value. This value is determined interactively by an analyst. We recommend that image differencing is performed with red, near-infrared, and NDVI image layers. Resulting change areas determined by thresholding and classifying the three image layers can be combined into a single change/no change image. Additional, but more time intensive change detection approaches are described in Coulter et al., 2003.

Image-based change detection identifies individual pixels and clusters of pixels that are likely to have changed, but does not delineate change polygons. As discussed previously, automated routines for delineating polygons can be iterative and do not always provide the desired result. The most efficient approach for delineating change polygons is likely to be through "heads-up" digitizing of polygons onto the change detection image. These polygons may then be used for subsequent analysis of habitat quality and change.

6.4 Image-Based Land Cover Analysis

Identified change areas may be investigated using field reconnaissance and/or image processing techniques described previously. The most efficient and objective image processing approach for quantifying the percent cover of shrub, herbaceous, and bare within each multitemporal image set is through classification of single date imagery using the Expert Classifier. An Expert Classifier model using single date imagery (as describe in Appendix B) may be applied to each of the multitemporal image sets, and resulting cover proportions may be compared to assess the overall change in habitat condition within the change polygons. Provided that the multitemporal image sets are radiometrically normalized and illumination/terrain shadowing differences are not extreme, a single set of parameters may be utilized to classify each image set in the Expert Classifier. Use of a single set of parameters for classifying each multitemporal image set reduces potential analyst bias that may result if unique parameter values were selected for each image set.

Determining the parameters to be utilized within Expert Classifier models will require iterative calibration with reference data. Reference data may be derived from detailed maps of vegetation type and cover distributions. Reference data may also be field collected. In this study, image classifications were calibrated based upon the percent cover of shrub, herbaceous, and bare cover within reference vegetation stand polygons. It may be more appropriate for long-term monitoring to calibrate cover type classifications using individual pixels or groups of pixels that correspond to specific, identifiable features within the project area. These features should represent a variety of shrub, herbaceous, and bare cover types.

7.0 References

Coulter, L., D. Stow, A. Hope, J. O'Leary, J. Franklin, A. Johnson, E. Witztum, A Petersen, P. Longmire, A. Wall, J Rogan, and E. Almanza, 2003. Regional Change Monitoring of Habitat Reserve Systems with Very High Resolution Remotely Sensed Data. NASA Earth Science Directorate Final Report, Food and Fiber Applications of Remote Sensing, Grant # NAG13-99017, 173 pp. [available in PDF format online at *http://typhoon.sdsu.edu/People/Pages/stow/SDSU_FFARS_Final_Report.pdf*]

Keeley, J.E. 2000. Chaparral. In: M.G. Barbour and W.D. Billings (eds.). *North American Terrestrial Vegetation.* 2nd Edition. Cambridge University Press.

O'Leary, J.F. 1990. Californian Coastal Sage Scrub: General Characteristics and Considerations for Biological Conservation. In: A.A. Schoenherr (ed.). *Endangered Plant Communities of Southern California.* Proceedings of the 15th Annual Symposium, Southern California Botanists, Special Publication No. 3, p. 24-41.

Story, T. T. 2000. 2000 MSCP Annual Public Workshop – Summary Report.

Myneni, R. B., F. G. Hall, P. J. Sellers, and A. L. Marshak. 1995. The Interpretation of Spectral Vegetation Indexes. *IEEE Transactions on Geoscience and Remote Sensing*, 33(2): 481-286.

Phinn, S., J. Franklin, A. Hope and D. Stow. 1996. Biomass Distribution Mapping Using Airborne Digital Video Imagery and Spatial Statistics in a Semi-arid Environment, *Journal of Environmental Management*, 47: 139-164..

Phinn, S., D. Stow, and D. Van Mouwerik. 1999. Remotely Sensed Estimates of Vegetation Structural Characteristics in Restored Wetlands, Southern California. *Photogrammetric Engineering and Remote Sensing*, 65(4): 485-493.

Appendix A. A Frame Center Matching Technique for Precise Registration of Multitemporal Airborne Frame Imagery

Appendix B. Rule-Based Image Classification in the Expert Classifier

Appendix C. Semi-Automated Delineation of Vegetation Stands through Image Segmentation

Appendix D. Image Classifications of Ground Cover at Marron Valley

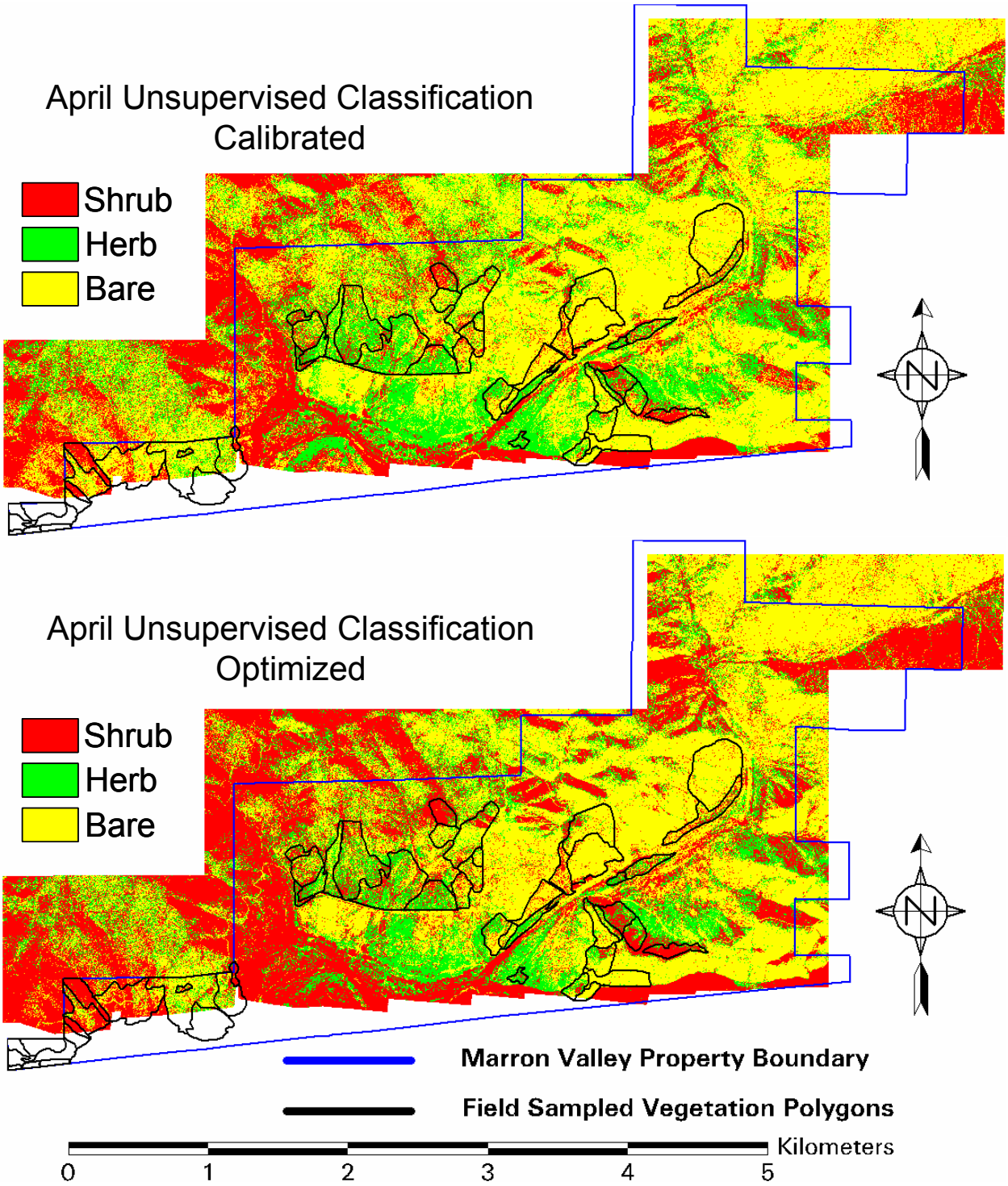

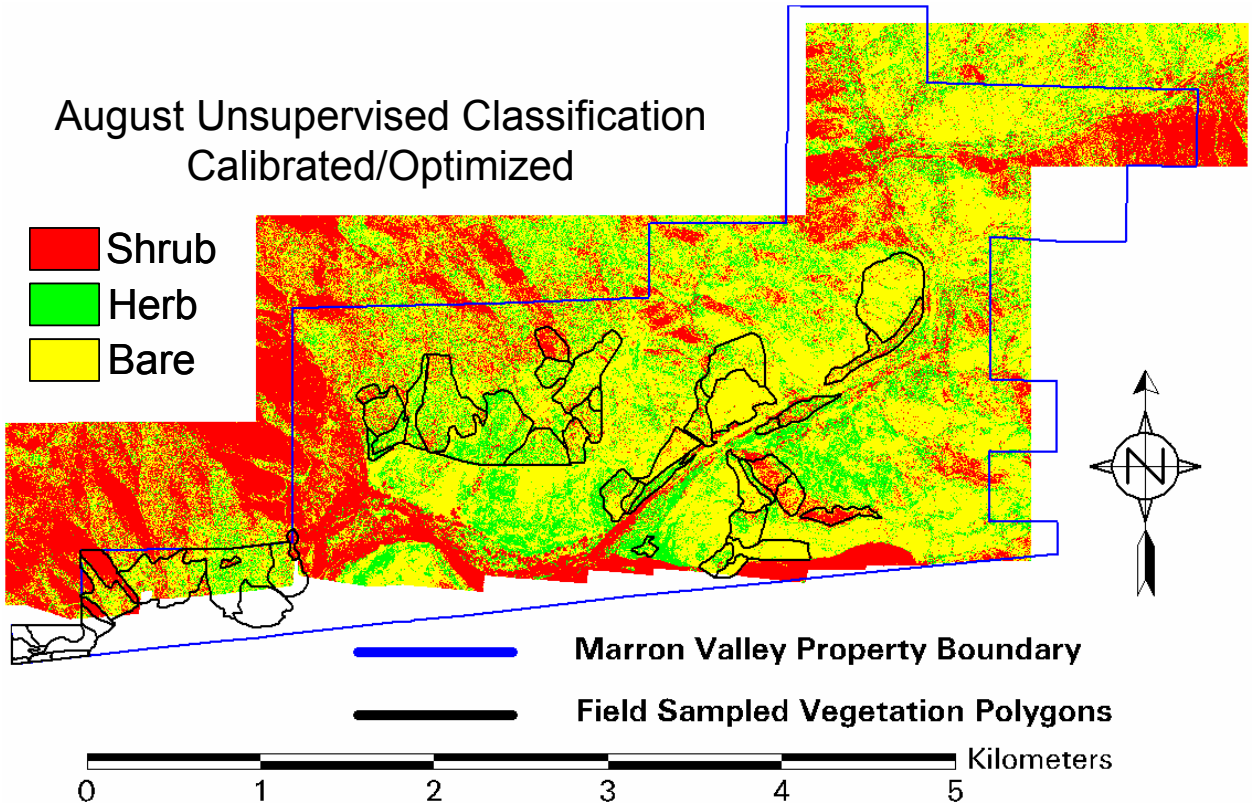
August Unsupervised Classification
Calibrated/Optimized
Shrub
Herb
Bare
N
Marron Valley Property Boundary
Field Sampled Vegetation Polygons
Kilometers
0
1
2
3
4
5

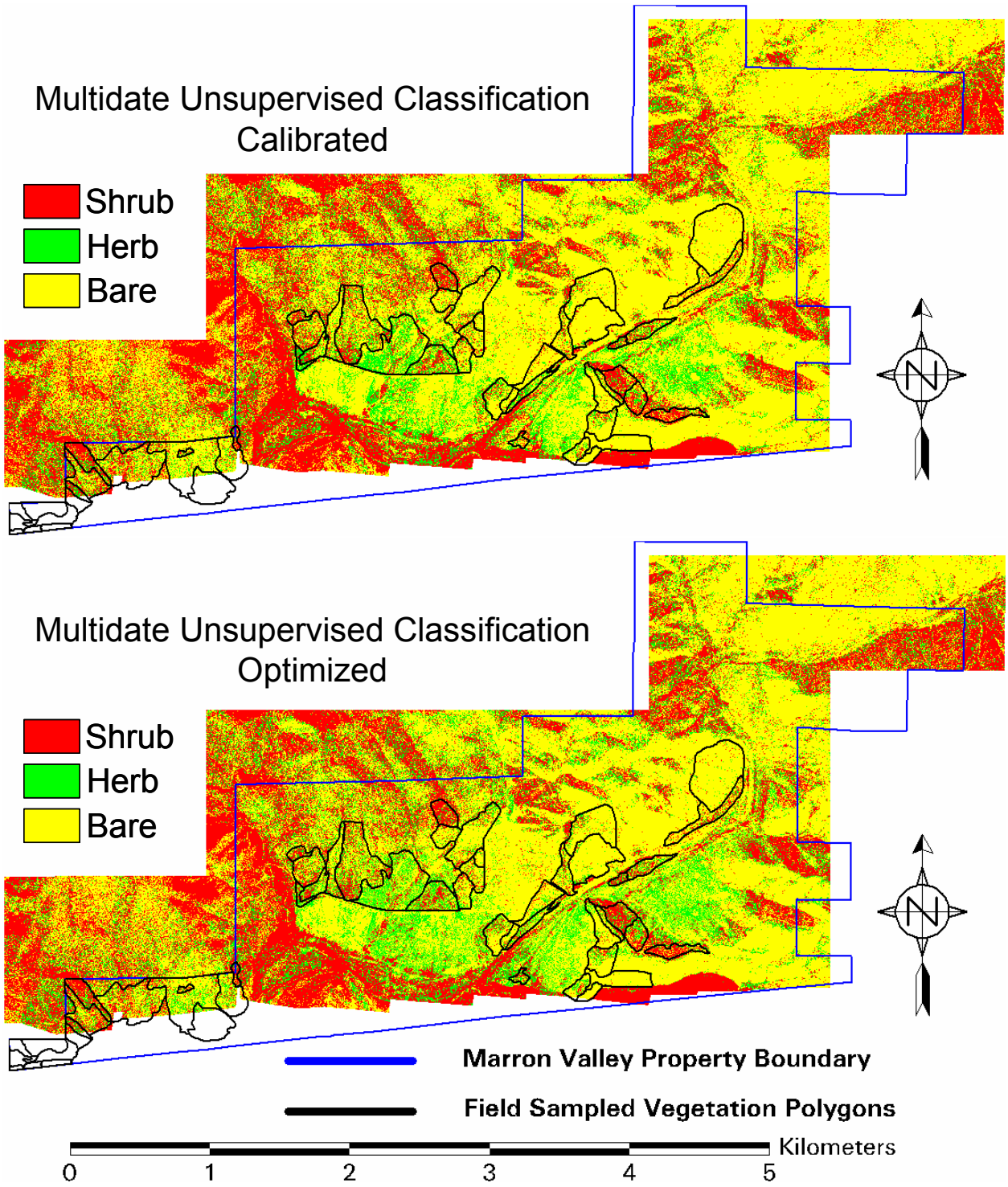
Multidate Unsupervised Classification
Calibrated
Shrub
Herb
Bare
N
Multidate Unsupervised Classification
Optimized
Shrub
Herb
Bare
N
Marron Valley Property Boundary
Field Sampled Vegetation Polygons
Kilometers
0
1
2
3
4
5

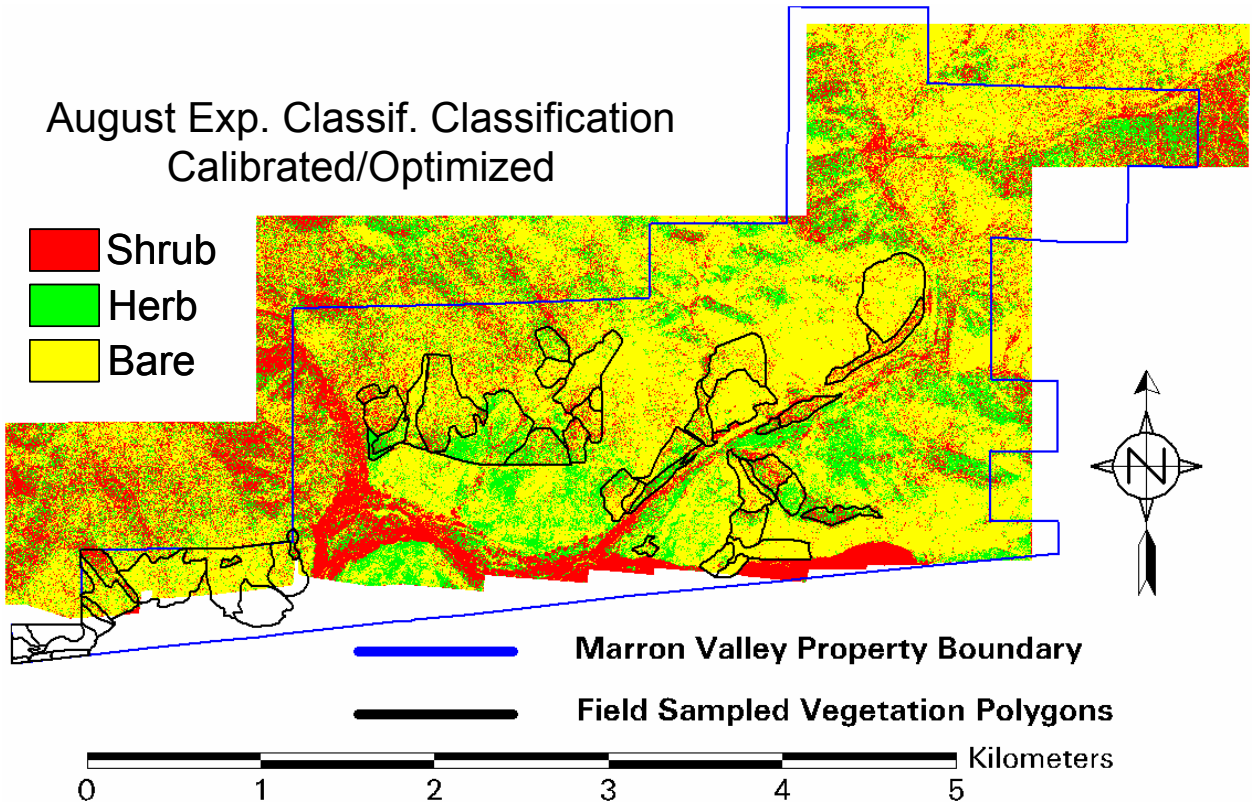
August Exp. Classif. Classification
Calibrated/Optimized
Shrub
Herb
Bare
N
Marron Valley Property Boundary
Field Sampled Vegetation Polygons
Kilometers
0
1
2
3
4
5

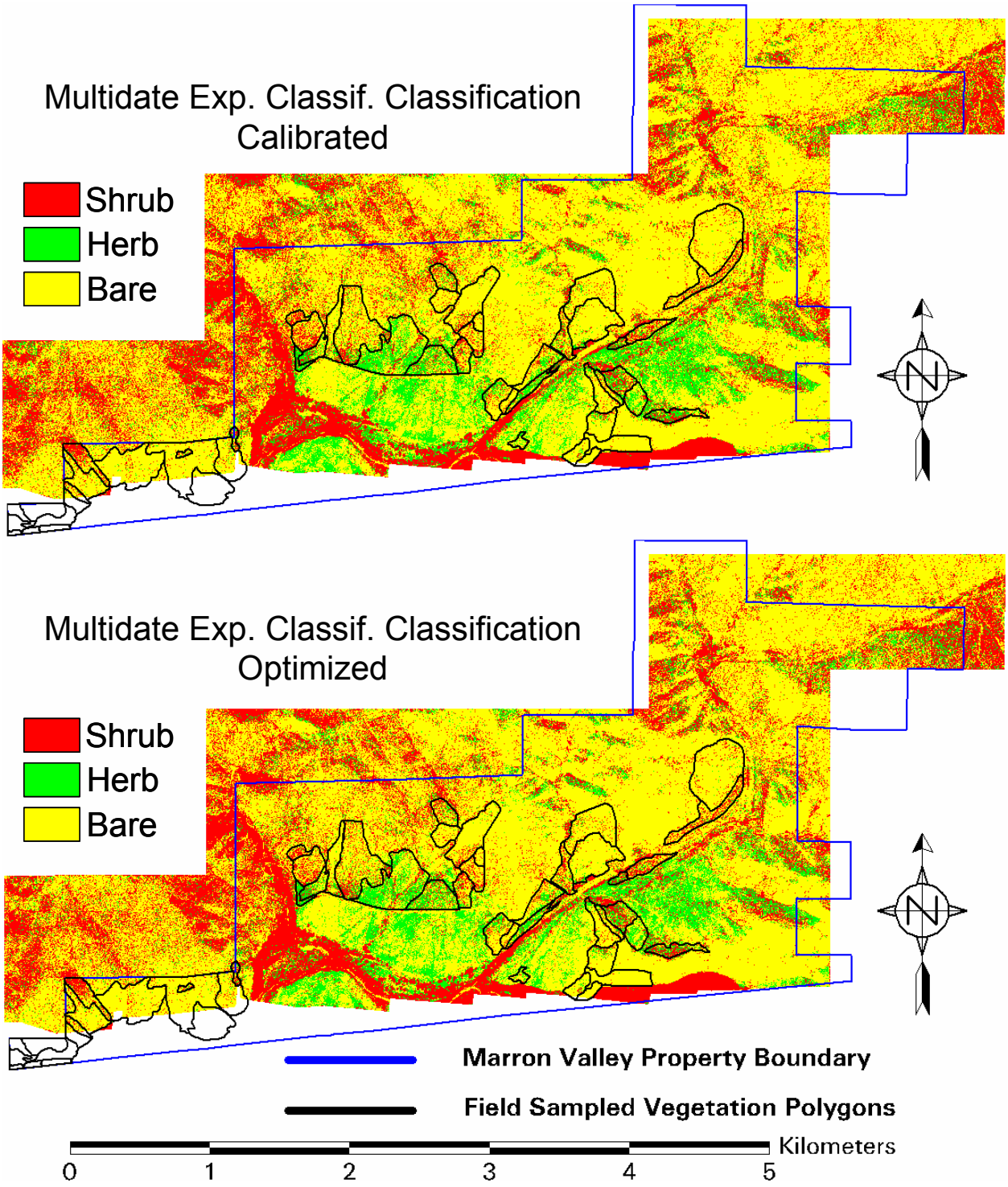
Multidate Exp. Classif. Classification
Calibrated
Shrub
Herb
Bare
N
Multidate Exp. Classif. Classification
Optimized
Shrub
Herb
Bare
N
Marron Valley Property Boundary
Field Sampled Vegetation Polygons
Kilometers
0
1
2
3
4
5

Appendix E. Scatterplots of Image-Derived Ground Cover Percentages versus Field Estimated Cover Percentages

Scatterplots illustrated here enable interpretation of model overestimation, underestimation, and random error of cover proportions derived through image classification, relative to cover proportions estimated in the field by City personnel. Scatterplots are given for calibrated and optimized versions of each classification.

Scatterplots for calibrated image classifications are given for the 10 polygon sample set that was used for calibration (illustrates the overall quality of the calibration), and the 35 polygons that were used as independent validation of the calibrated image classifications.

Scatterplots for optimized image classifications illustrate validation for the full set (all 45 polygons), all of which were used to calibrate the optimized image classifications. Optimized image classification were generated to assess the potential accuracy of image classifications given all available information on vegetation cover within the scene. Optimized image classifications are expected to represent the limit of classification accuracy that is obtainable from 1 m multispectral imagery. In addition to providing scatterplots showing the agreement of cover proportions for all 45 polygons used in this study, scatterplots are graphed for the 10 calibration polygons separately, so that the effect of optimizing the image classifications on the calibration polygons may be reviewed.

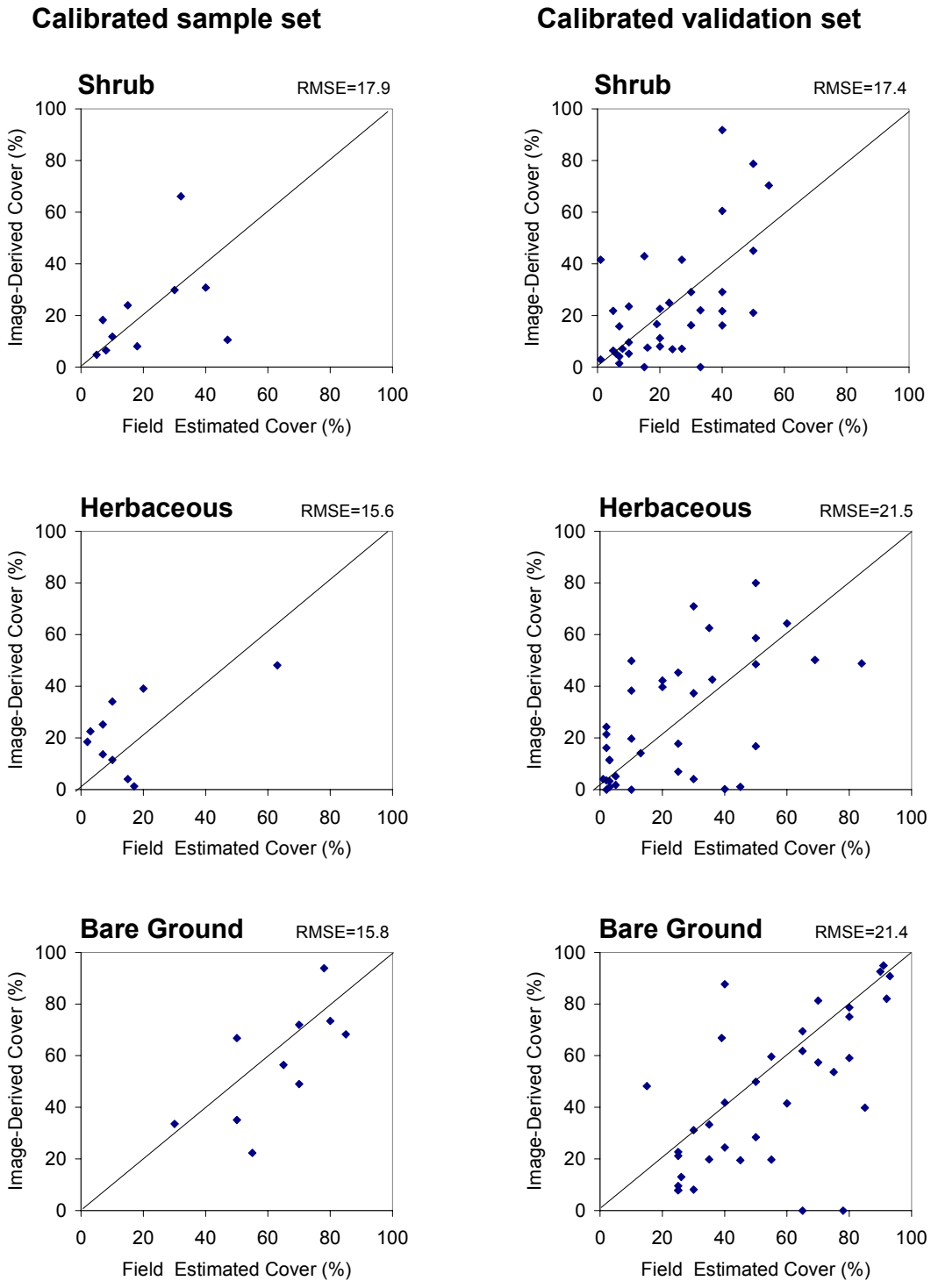

April Unsupervised Classification (using NDVI) – CALIBRATED
RMSE = root mean square error

Optimized full set

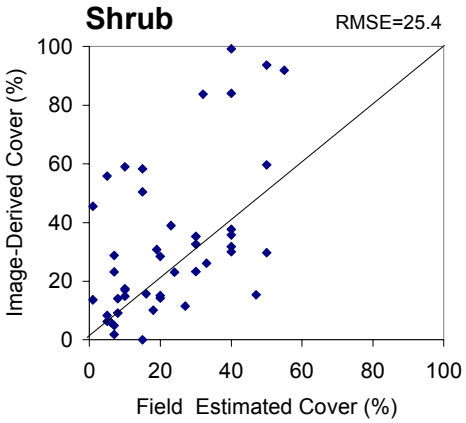

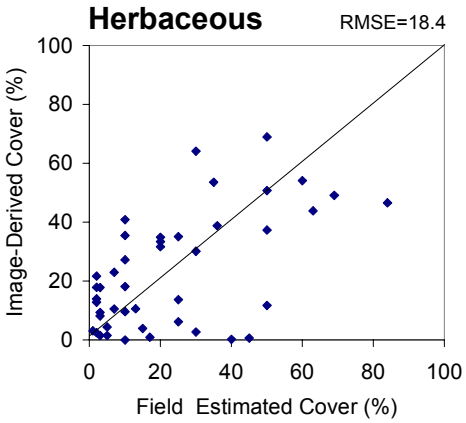

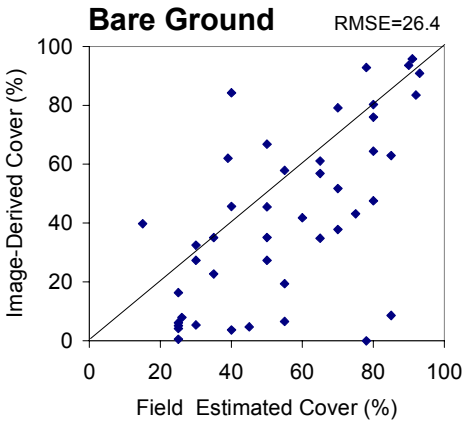

Optimized sample set

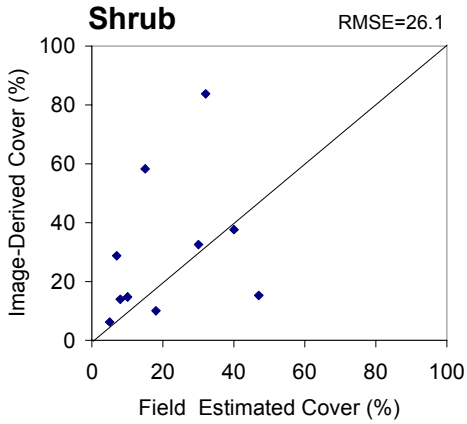

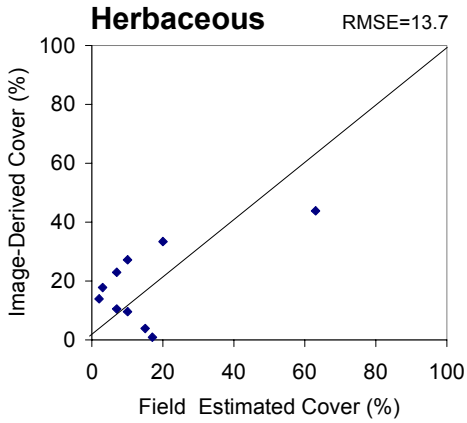

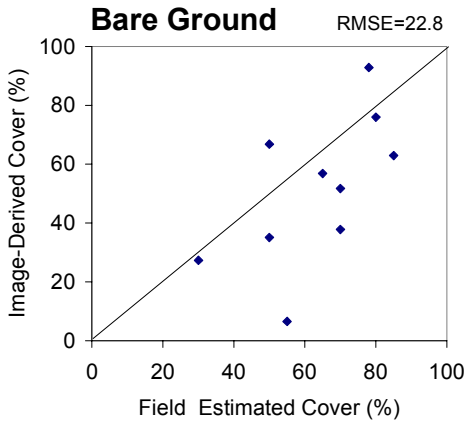

April Unsupervised Classification (using NDVI) - OPTIMIZED
RMSE = root mean square error

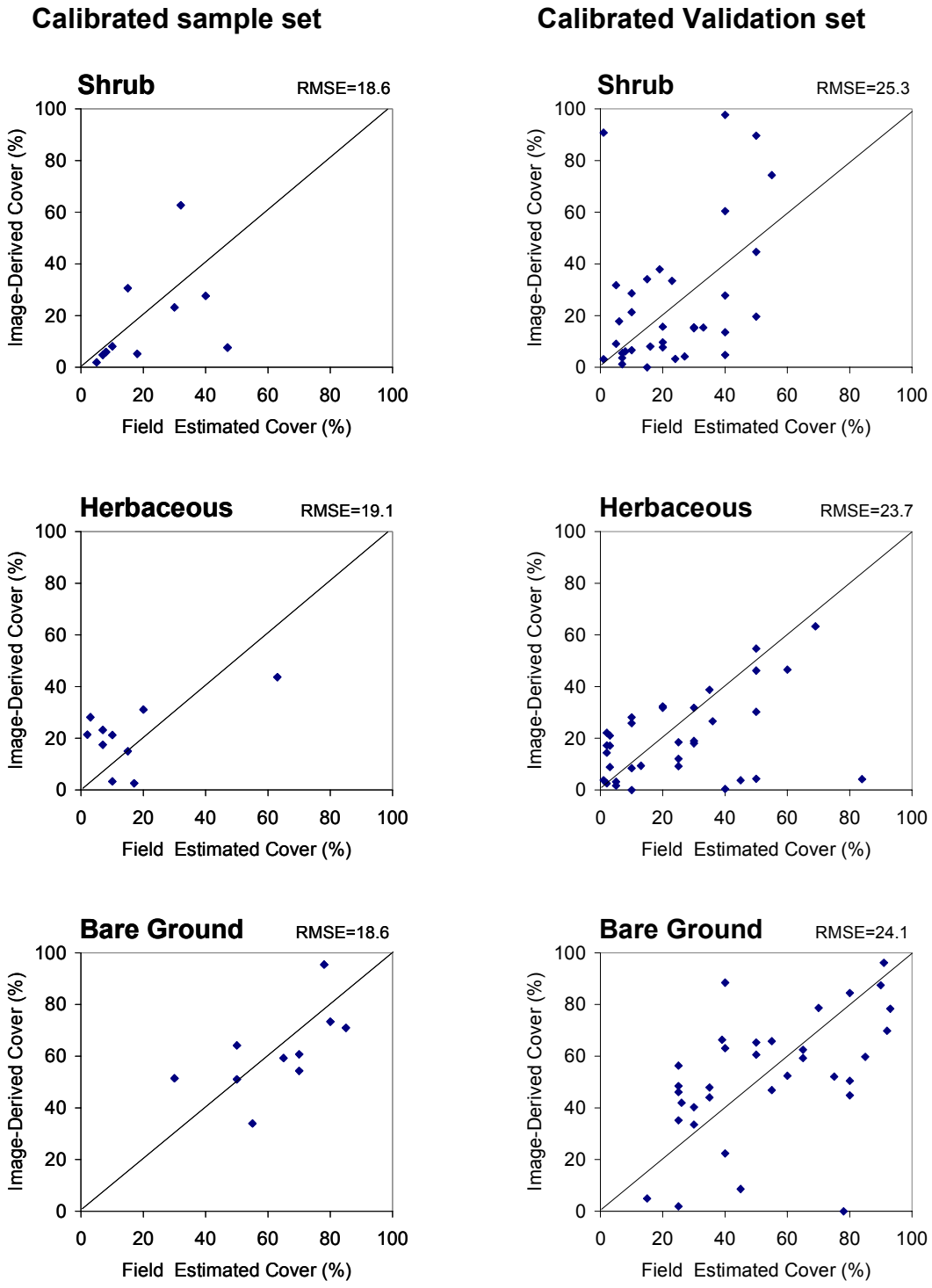

August Unsupervised Classification (using NDVI) – CALIBRATED
RMSE = root mean square error

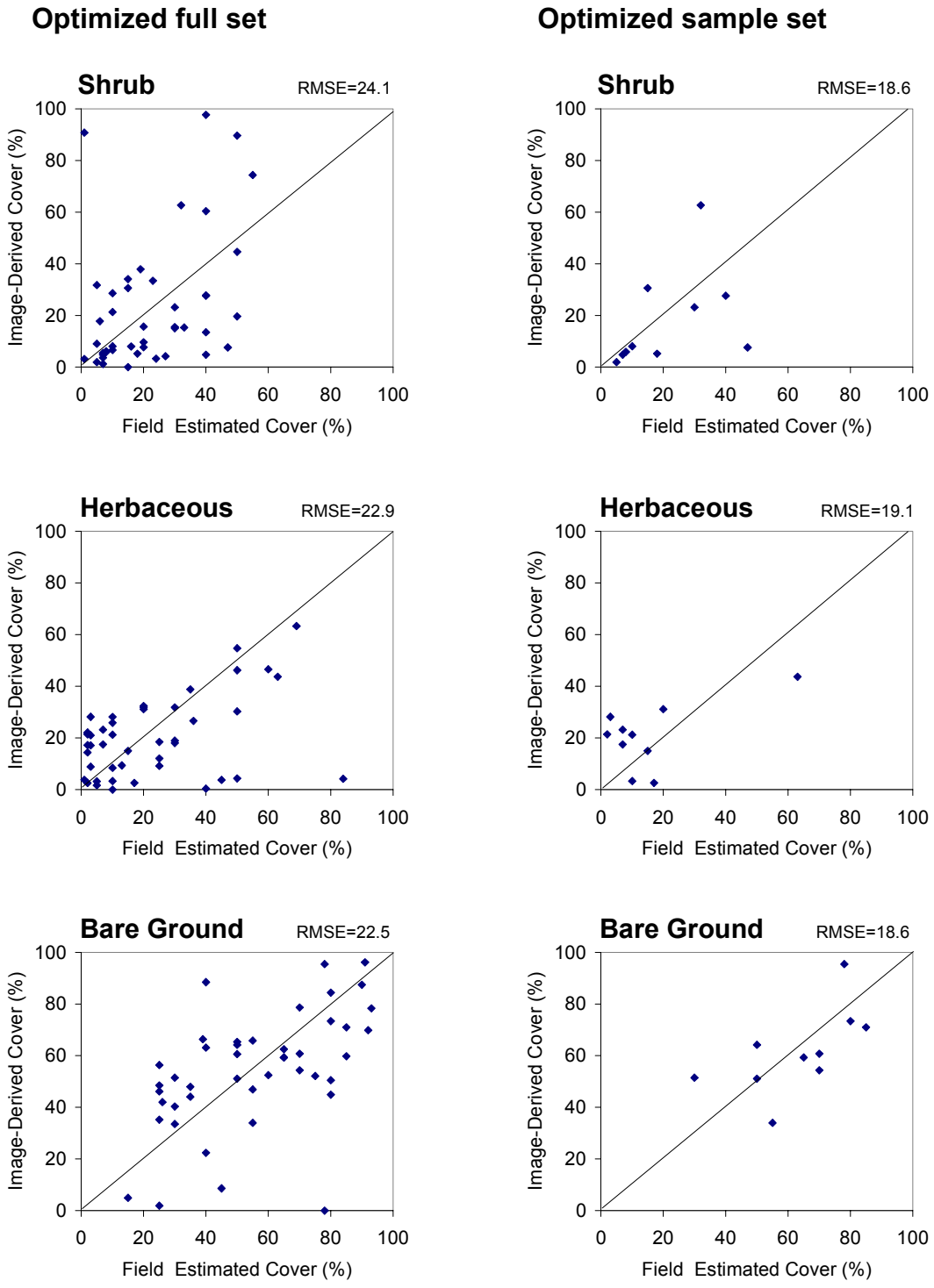

August Unsupervised Classification (using NDVI) – OPTIMIZED
RMSE = root mean square error

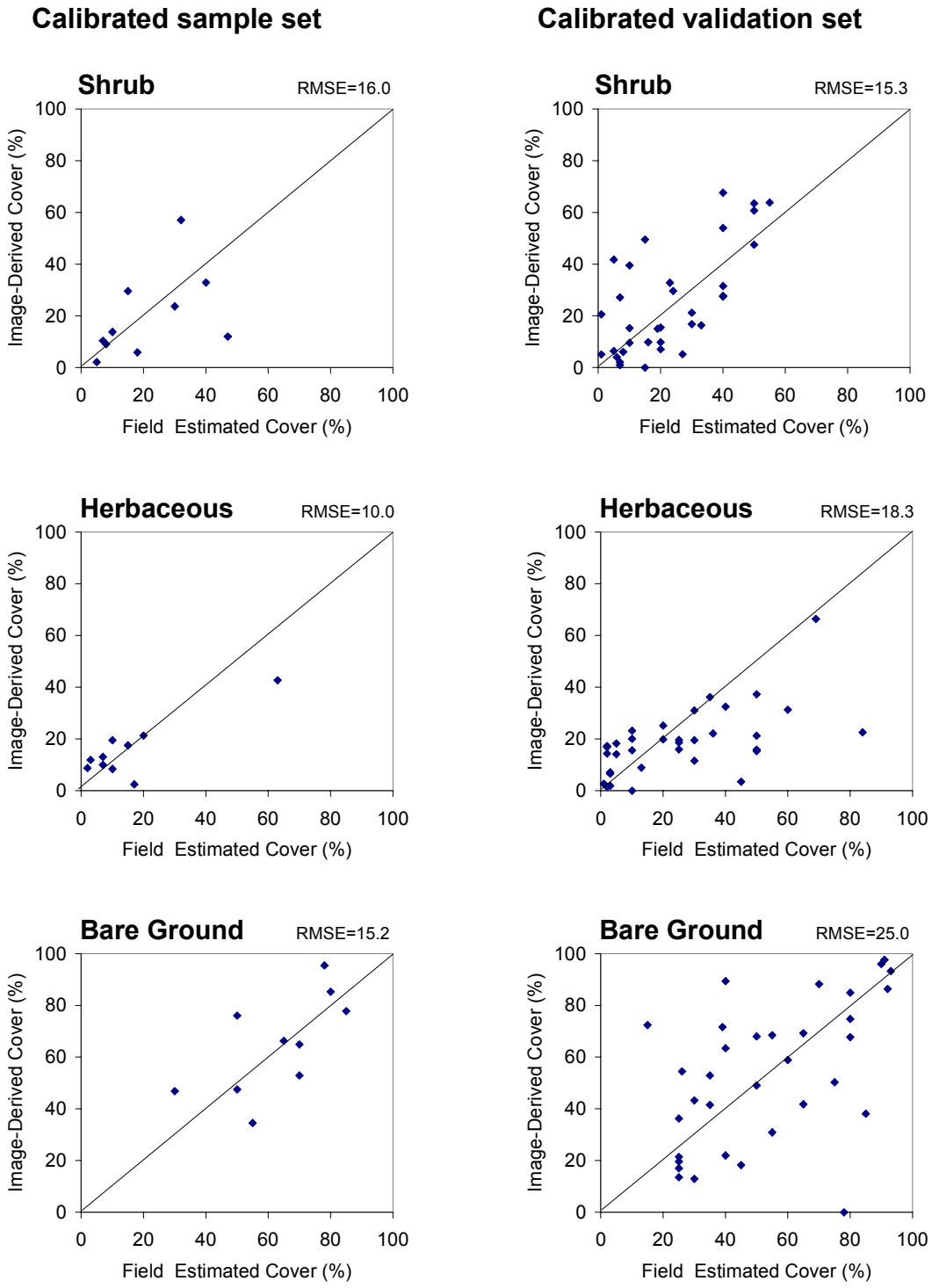

Multidate Unsupervised Classification (using NDVI) – CALIBRATED
RMSE = root mean square error

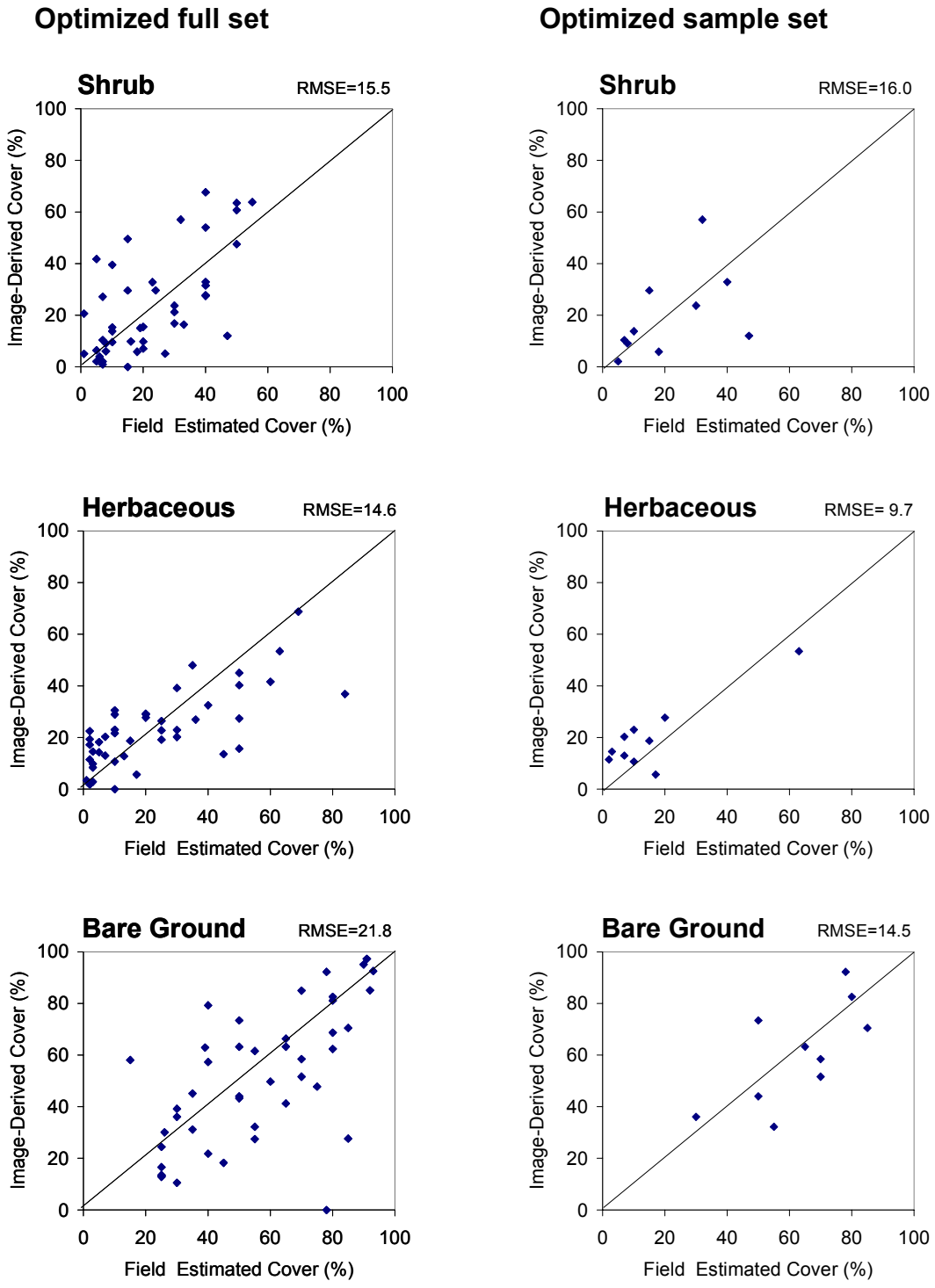

Multidate Unsupervised Classification (using NDVI) – OPTIMIZED
RMSE = root mean square error

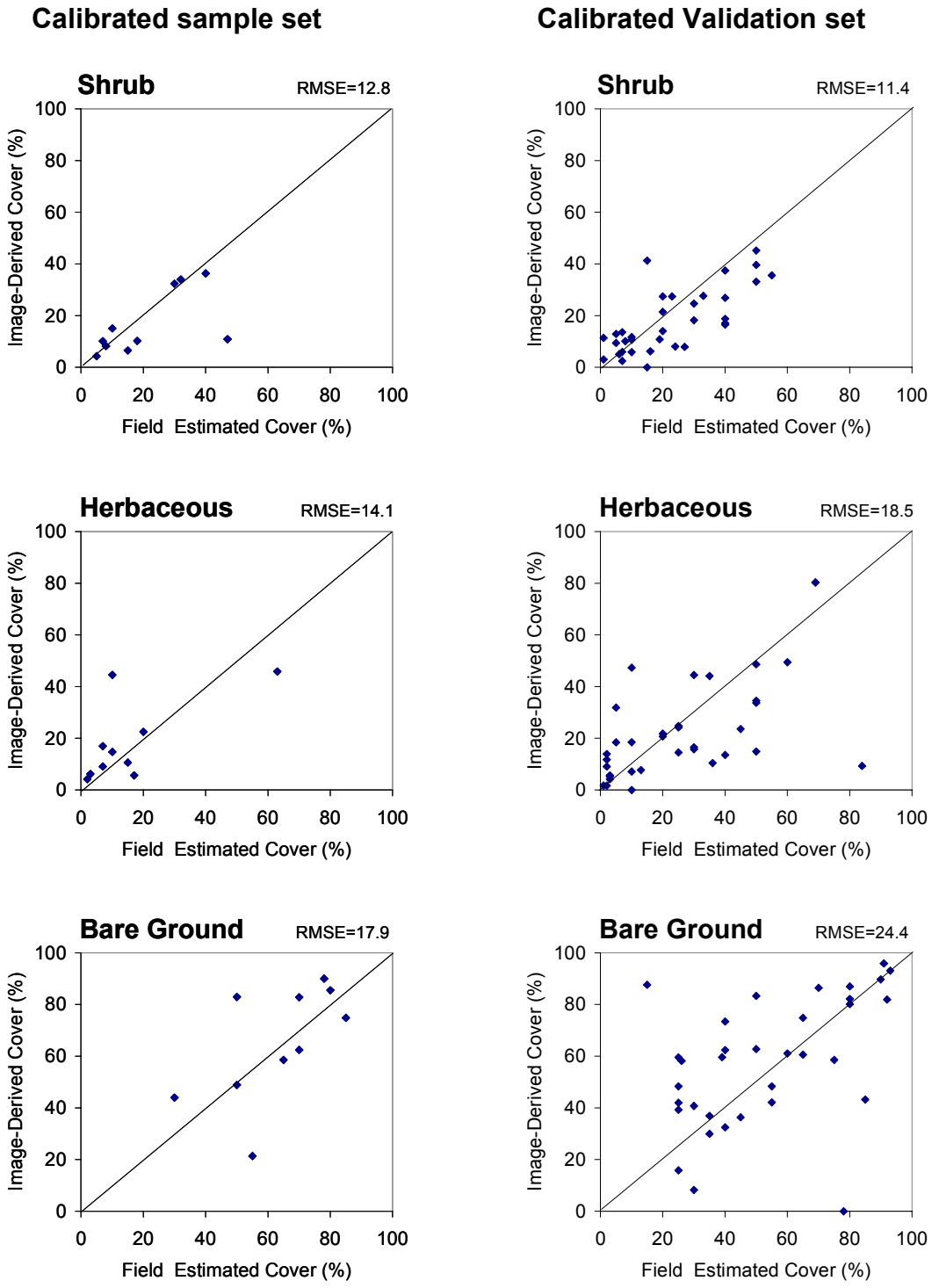

August Expert Classifier Classification – CALIBRATED
RMSE = root mean square error

Optimized full set

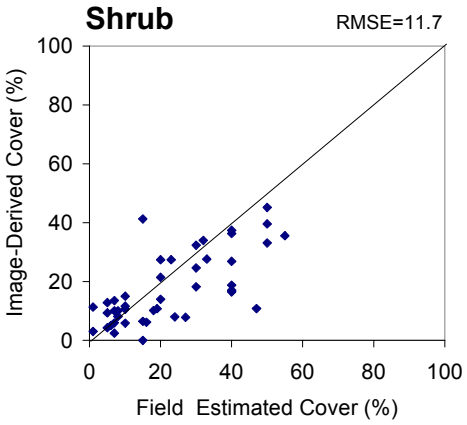

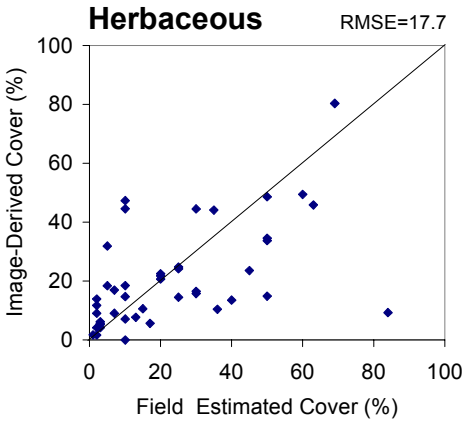

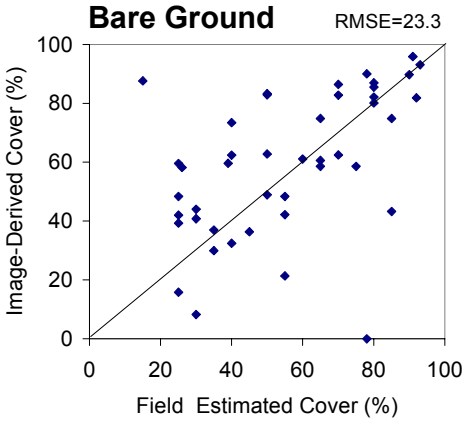

Optimized sample set

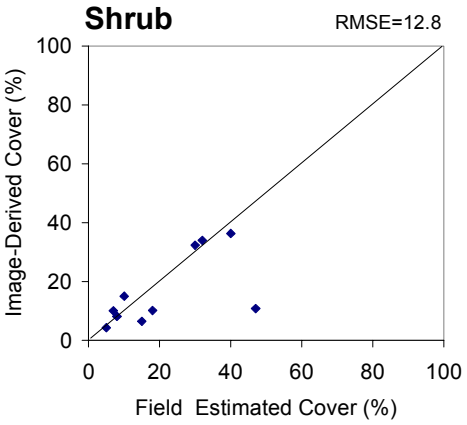

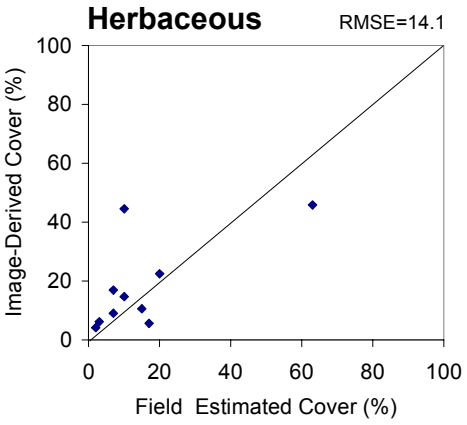

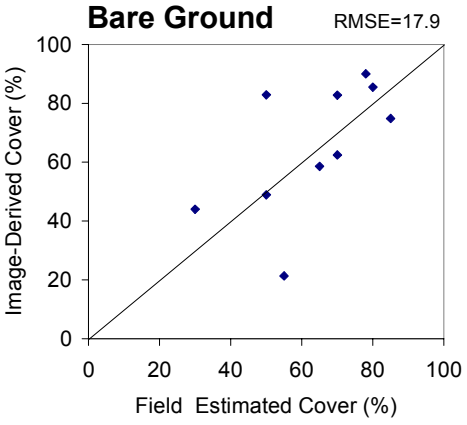

August Expert Classifier Classification – OPTIMIZED
RMSE = root mean square error

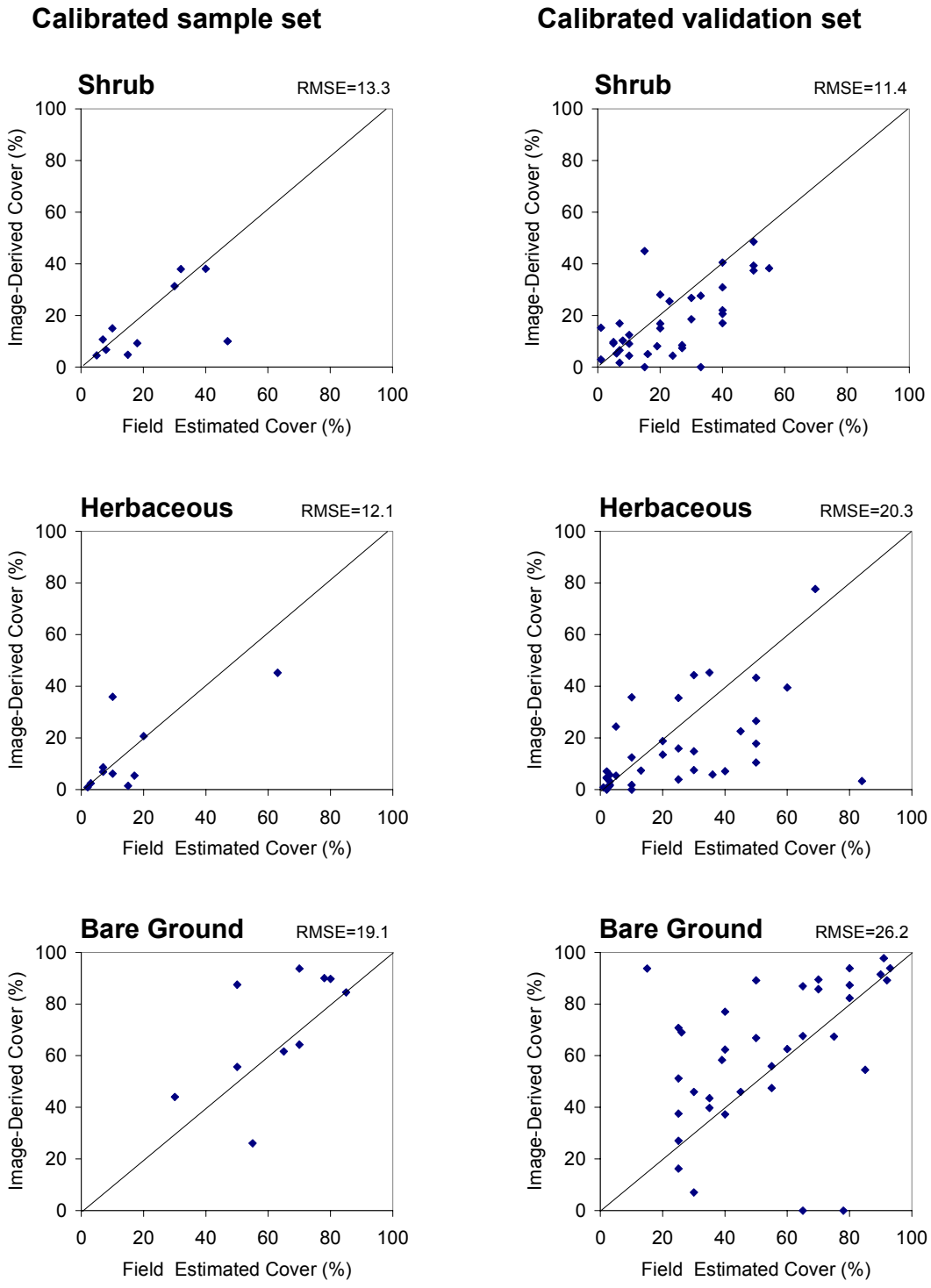

Multidate Expert Classifier Classification – CALIBRATED
RMSE = root mean square error

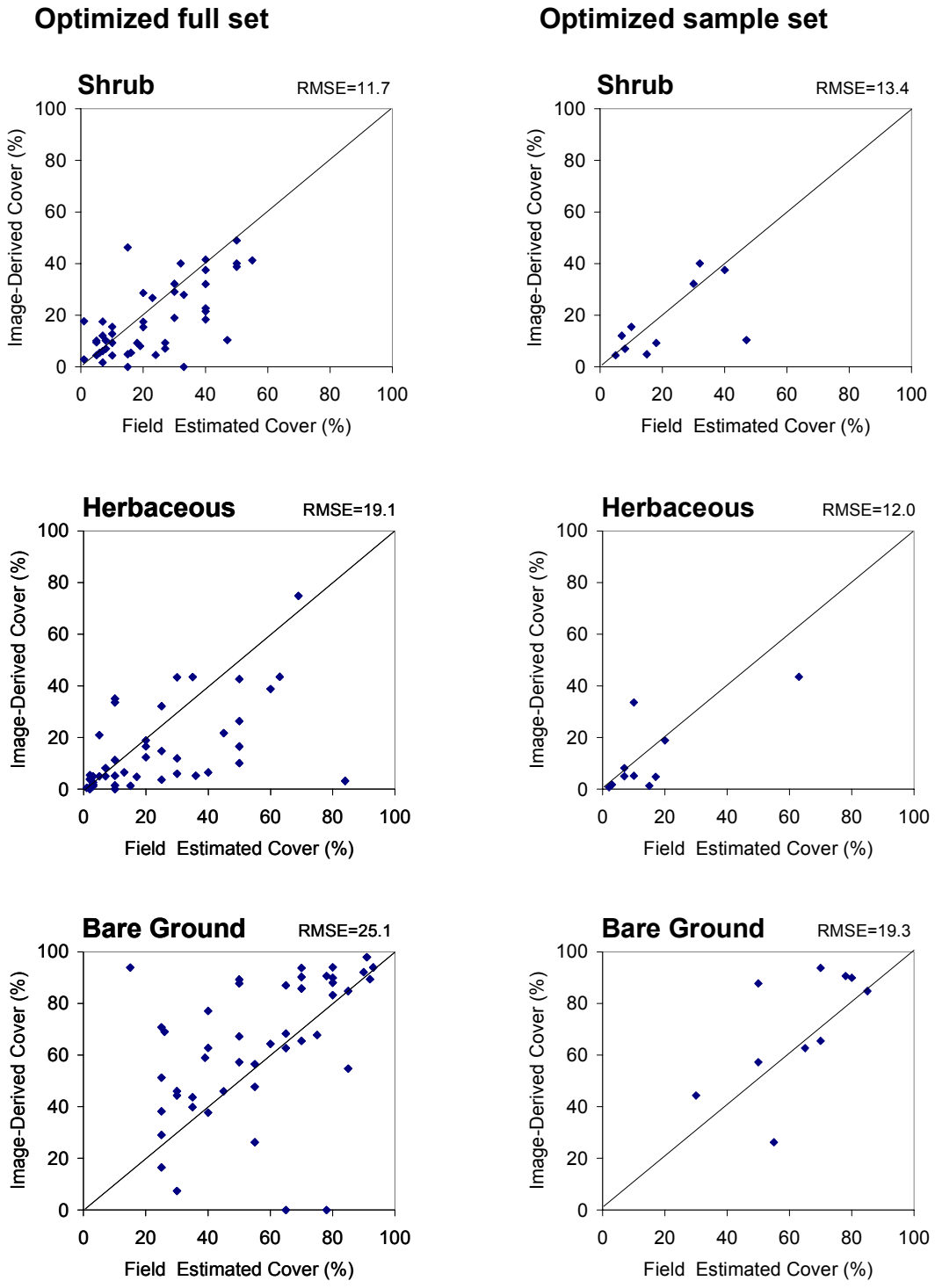

Multidate Expert Classifier Classification – OPTIMIZED
RMSE = root mean square error